Indian Summer Monsoon Simulation:Convection schemes

P. Mukhopadhyay

Contributing scientists: Medha Deshpande, Phani Murli Krishna, Mata Mahakur, Malay Ganai, Kumar Roy ,Radhik Kanase, Bidyut Goswamia and Abhik S.

Outline

- Diurnal variation,daily and seasonal
- Issues with mass flux and adjustment closure
- Recent new approaches
- Summary

The Need for a Parameterisation

Convection is a sub-grid scale phenomenon. It cannot be explicitly computed (resolved) by an atmospheric model. Hence, it should be *parameterised*.

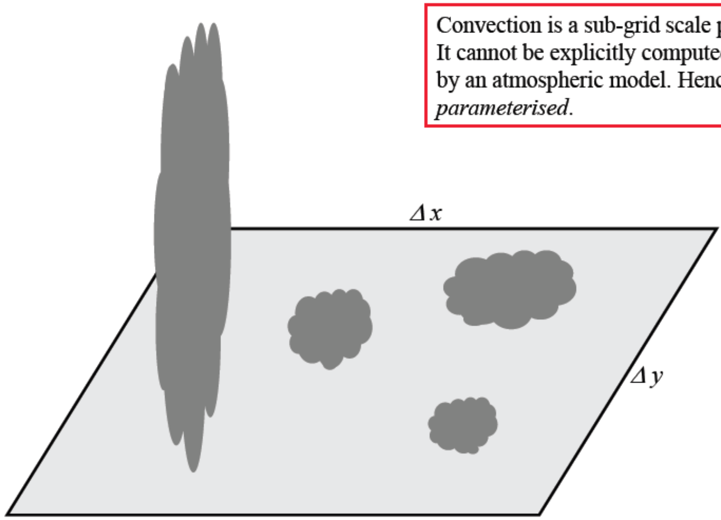

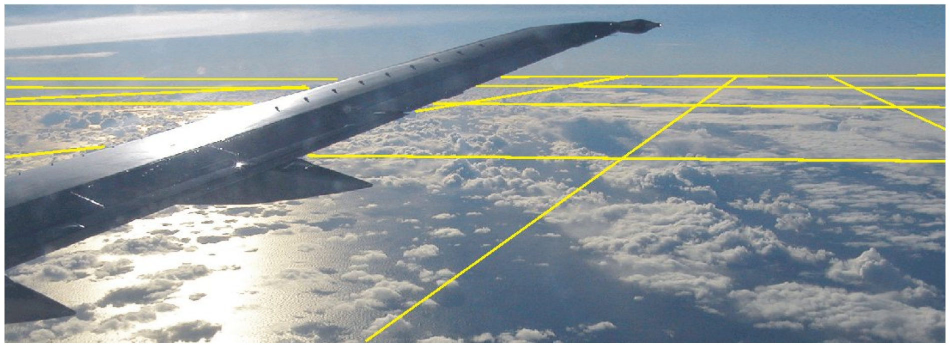

Clouds in GCMs - What are the problems ?

Many of the observed clouds and especially the processes within them are of subgrid-scale size (both horizontally and vertically)

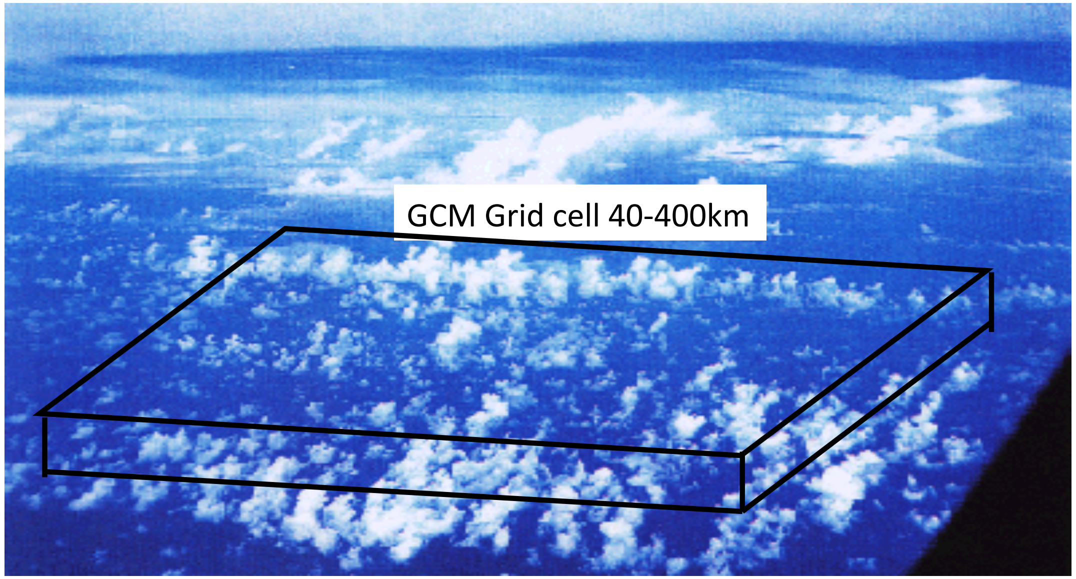

Phenomenology

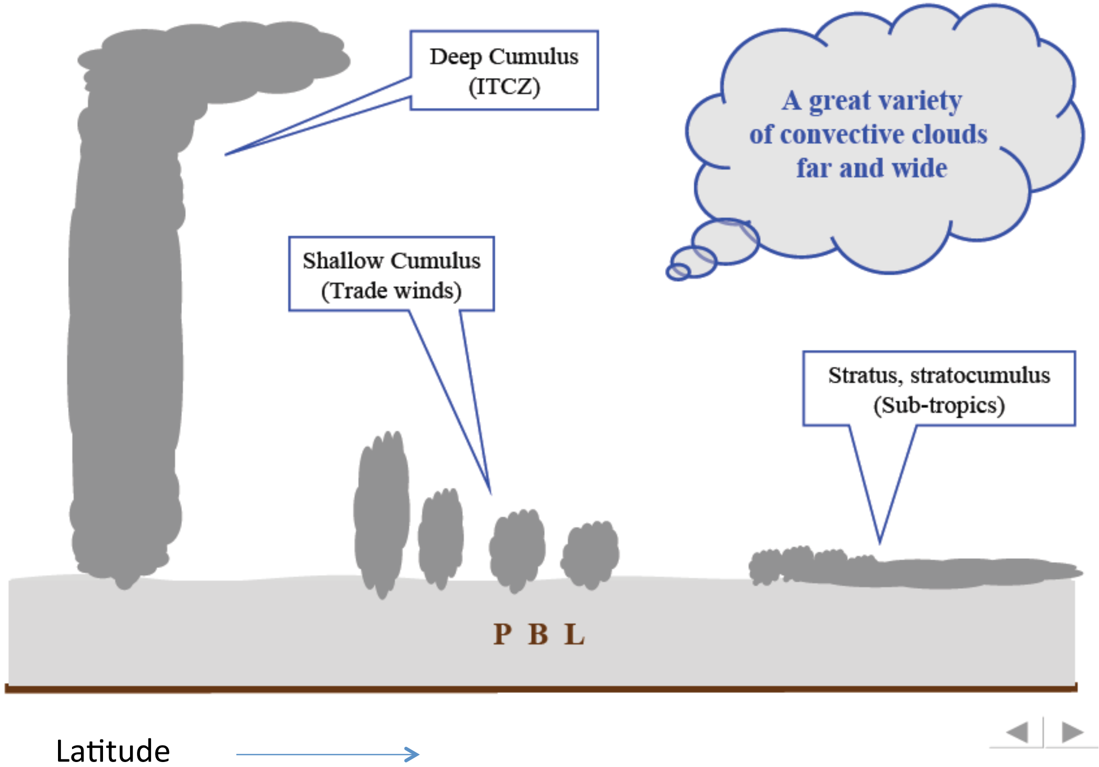

Han and Pan 2011

Revision of Convection and Vertical Diffusion Schemes in the NCEP Global Forecast System

JONGIL HAN

Wyle Information Systems LLC, and National Centers for Environmental Prediction/Environmental Modeling Center, Camp Springs, Maryland

HUA-LU PAN

National Centers for Environmental Prediction/Environmental Modeling Center, Camp Springs, Maryland

For deep convection, the scheme is revised to make cumulus convection stronger and deeper to deplete more instability in the atmospheric column and result in the suppression of the excessive grid-scale precipitation.

Large eddy simulation (LES) studies by Siebesma and Cuijpers (1995) indicate that the fractional entrainment and detrainment rates for the SC are one order of magnitude larger than the values used in most existing deep convection schemes. The LES study by Siebesma et al. (2003) indicates that a typical value for the fractional entrainment rate is $\varepsilon \sim 2.0 \times 10^{-3} m^{-1}$ near the cloud base, which agrees with other LES studies (Siebesma and Cuijpers 1995; Grant and Brown 1999) and observations (Raga et al. 1990), and that the entrainment rate behaves as

$$\varepsilon = c_e \frac{1}{z},$$

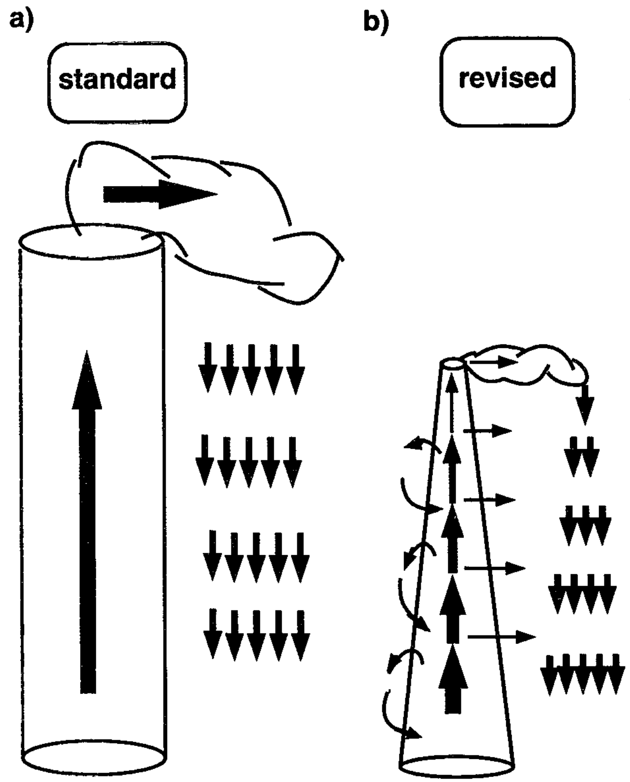

FIG. 7. Schematic picture of the turbulent mixing mechanism of a shallow cloud ensemble. In the case of the standard values of ϵ and δ, the scheme behaves approximately as a nonleaking funnel with massive detrainment at cloud top. When using the enhanced values of ϵ and δ, as suggested by the LES results, there is more intense lateral mixing and a decreasing mass flux with height due to the fact that $\delta > \epsilon$ and hence little massive detrainment at the top.

Model Impacts of Entrainment and Detrainment Rates in Shallow Cumulus Convection

A. P. SIEBESMA AND A. A. M. HOLTSLAG*

JAS, 1996

The mass flux decreases with height above the cloud base while it increases with height below the cloud base, which is consistent with the aforementioned LES studies.

The liquid water in the updraft layer is allowed to be detrained from every layer into the convective rain and grid-scale cloud water with conversion parameters of 0.002 m^{-1} and 5.0 x 10^{-4} m^{-1}, respectively.

The feedback of cumulus convection into the largescale environment is accomplished via the compensating subsidence in the environment and the entrainment and detrainment processes between the cloud and the environment.

Han and Pan 2011

"The CFS run was initialized at 0000 UTC 16 December 2002 and ran for 45 days. The CFS forecasts during the preceding 15 days (a spinup period) have been discarded from the analysis, and forecast results during the remaining 1-month period are presented. An evaluation using a longer CFS run would be desirable, but will be left for a future study."

Han and Pan 2011, WAF

A recent Review (Sept 2014) obtained on our analyses of CFSv2 T382 climate run

"My main point is that without modifying/optimizing the model physics for very high resolution, simply increasing the model resolution and generating long simulation is scientifically incorrect and useless.

Hence, before conducting various analysis with long term simulation data, it is very important to verify the physical robustness of the model physics and the biases observed in the simulation of BSISOs are not due to error coming from inappropriate use of model physics."

Parameterization is very much important but we can not wait for all the parameterization to reach its perfection before issuing high resolution forecast: Developement should continue and model should continue to get upgraded

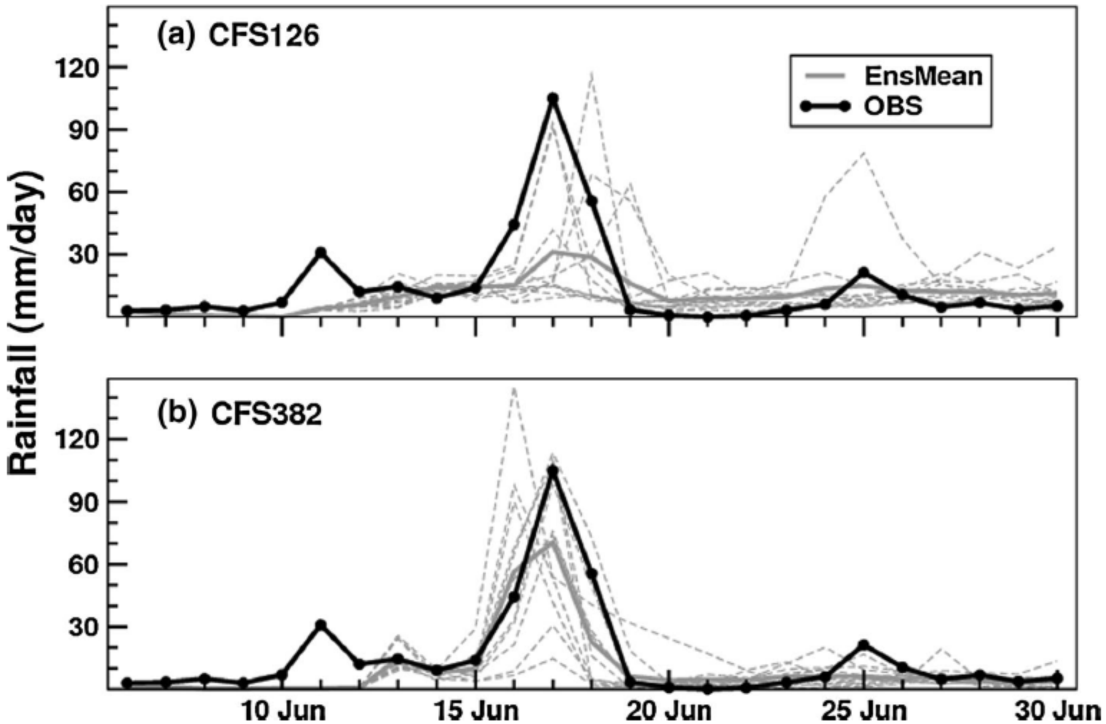

Extended range prediction of Uttarakhand rainfall event by a CFS126 and b CFS382 from 05 June initial condition. The region where rainfall values are averaged is 78°–80°E; 29°–31°N. Individual ensemble members are shown as dashed lines

Joseph et al., Clim. Dyn., Aug, 2014

REVOLUTIONIZING CLIMATE MODELING with PROJECT ATHENA:A Multi-Institutional, International Collaboration
by Kinter et al. BAMS, 2013

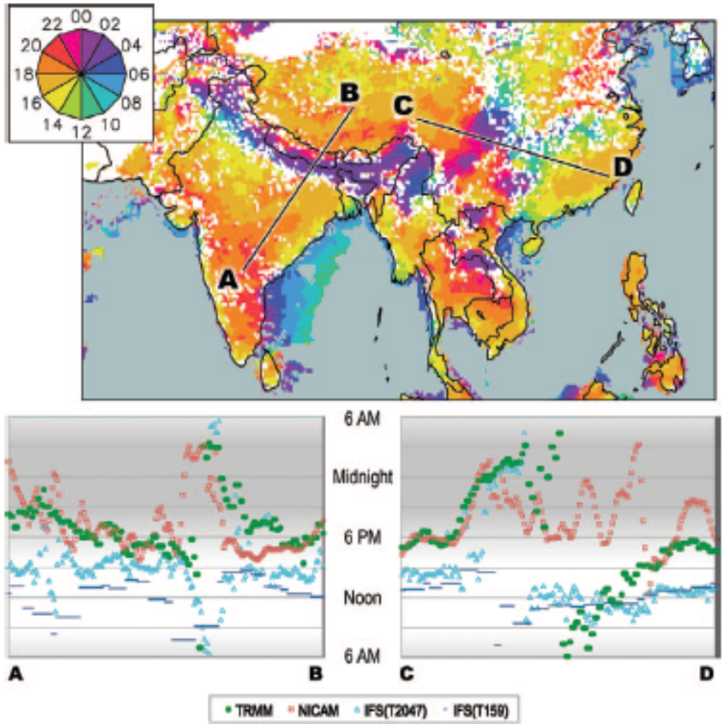

FIG. 7. Phase of the diurnal cycle of precipitation in observations and models. (top) The June–August mean hour of maximum rainfall estimated from TRMM data over 1998–2009. The colors correspond to local time on the 24-hour clock shown as an inset at the top left. (bottom) The hour of maximum rainfall for transects along lines (left) A–B and (right) C–D. Two transects are shown (A–B) and (C–D) for TRMM (green circles), NICAM (red squares), IFS 125-km simulation (blue dashes), and IFS 10-km simulation (cyan triangles). Data from all sources were first interpolated to the NICAM grid for ease of comparison. Values over ocean points where the amplitude of the diurnal cycle is less than half the seasonal mean (June–August) rainfall, and values over land points where the rainfall rate is less than 0.2 mm day^{-1} are not shown.

Diurnal phase corresponding to maximum precipitation

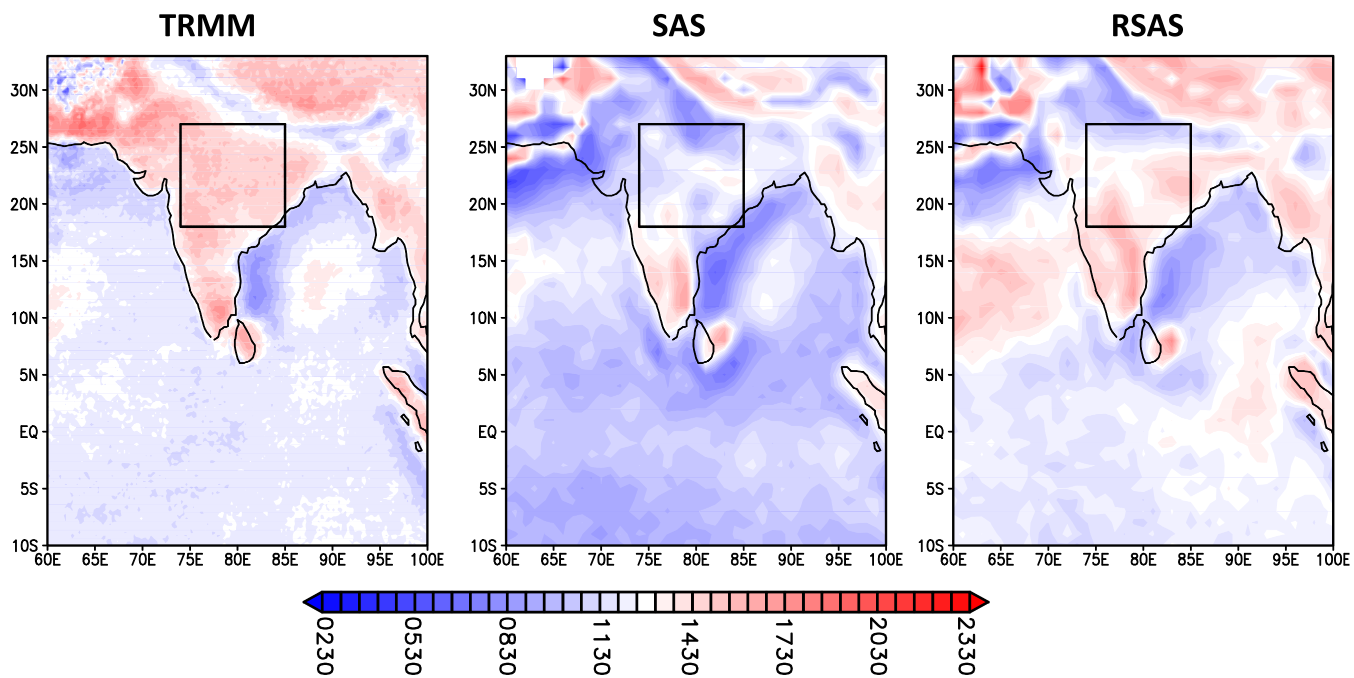

Black box represents Central India (CI) (18°N-27°N, 74°E-85°E) region

Diurnal absolute amplitude during JJAS

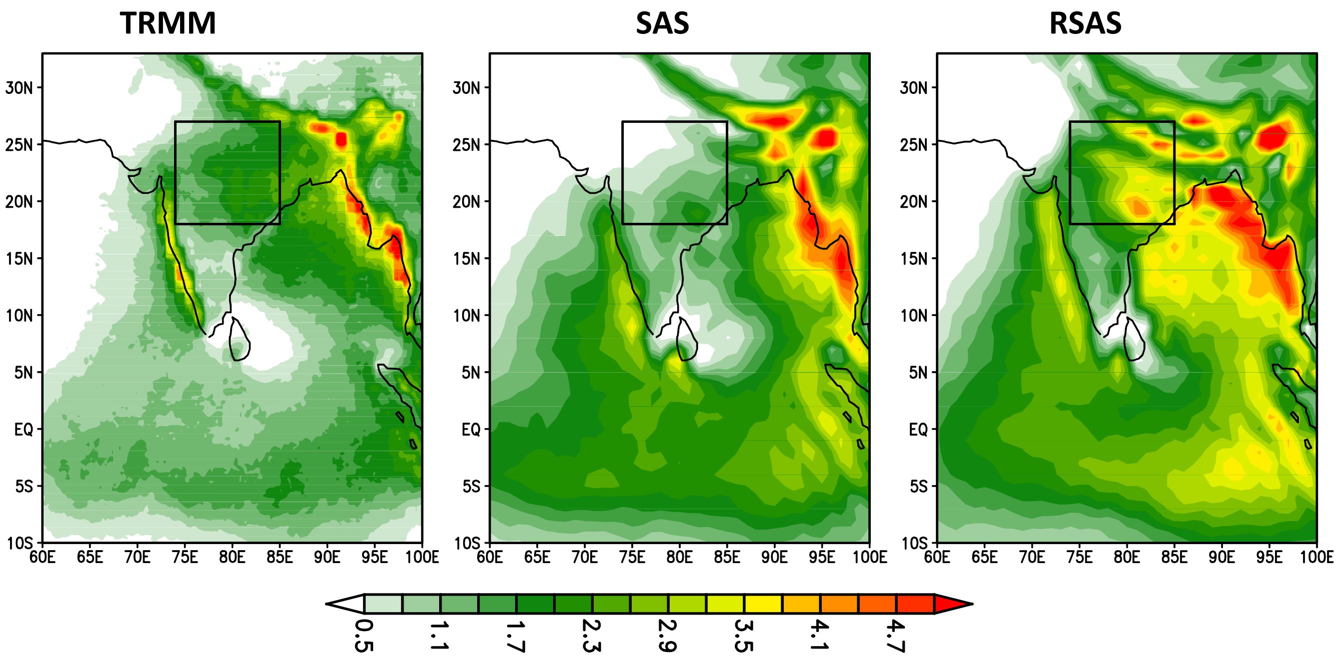

Black box represents Central India (CI) (18°N-27°N, 74°E-85°E) region

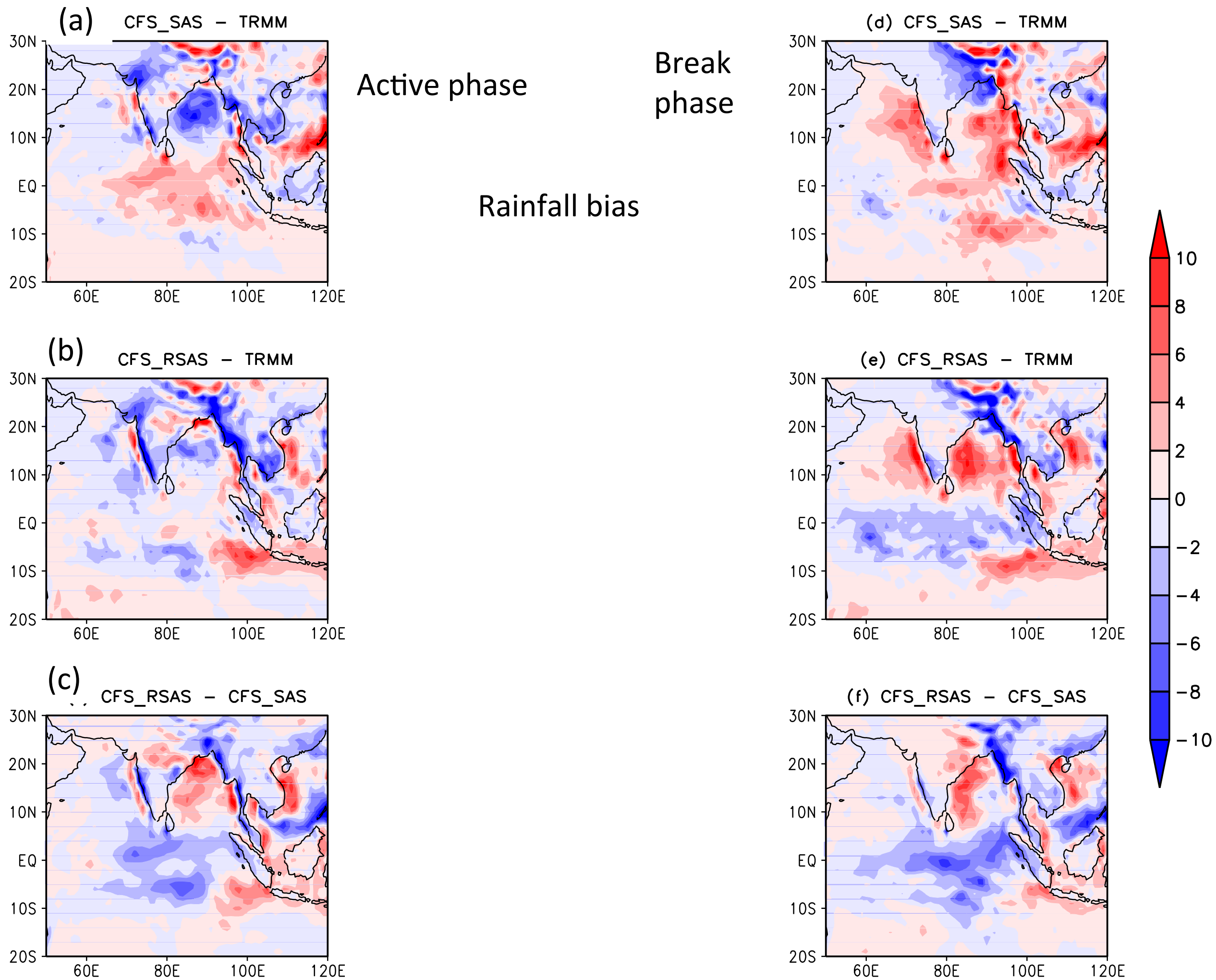

(a)
CFS_SAS – TRMM
Active phase
Break phase
Rainfall bias
(b)
CFS_RSAS – TRMM
(c)
CFS_RSAS – CFS_SAS
(d) CFS_SAS – TRMM
(e) CFS_RSAS – TRMM
(f) CFS_RSAS – CFS_SAS
30N
20N
10N
EQ
10S
20S
60E
80E
100E
120E
10
8
6
4
2
0
−2
−4
−6
−8
−10

Total rainfall PDF

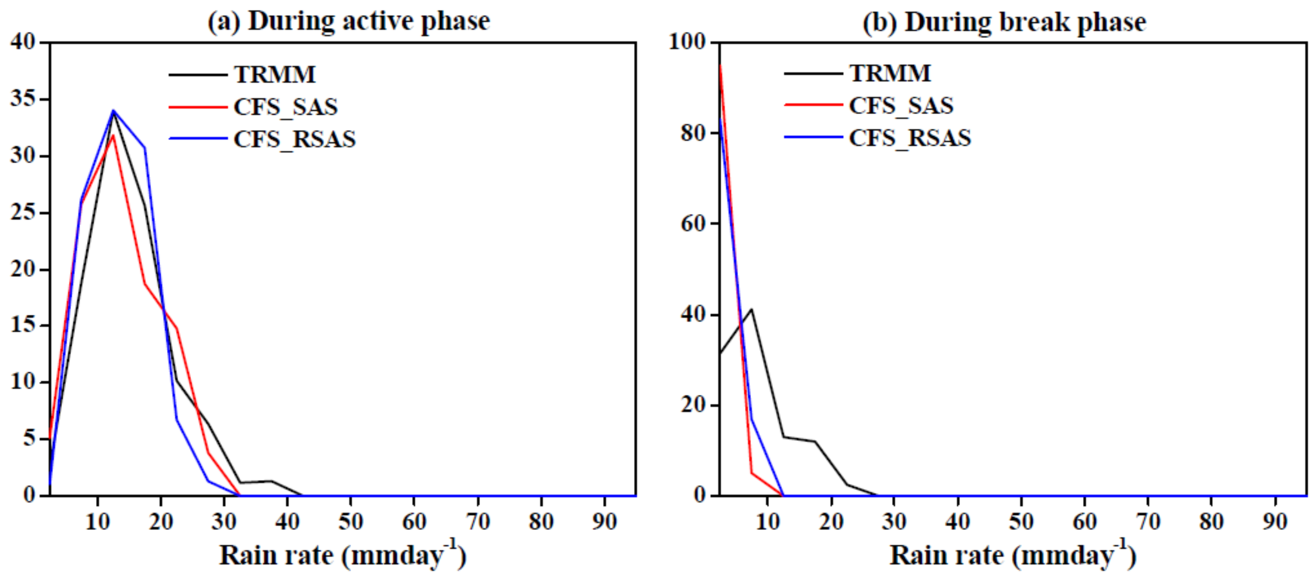

Convective rainfall PDF

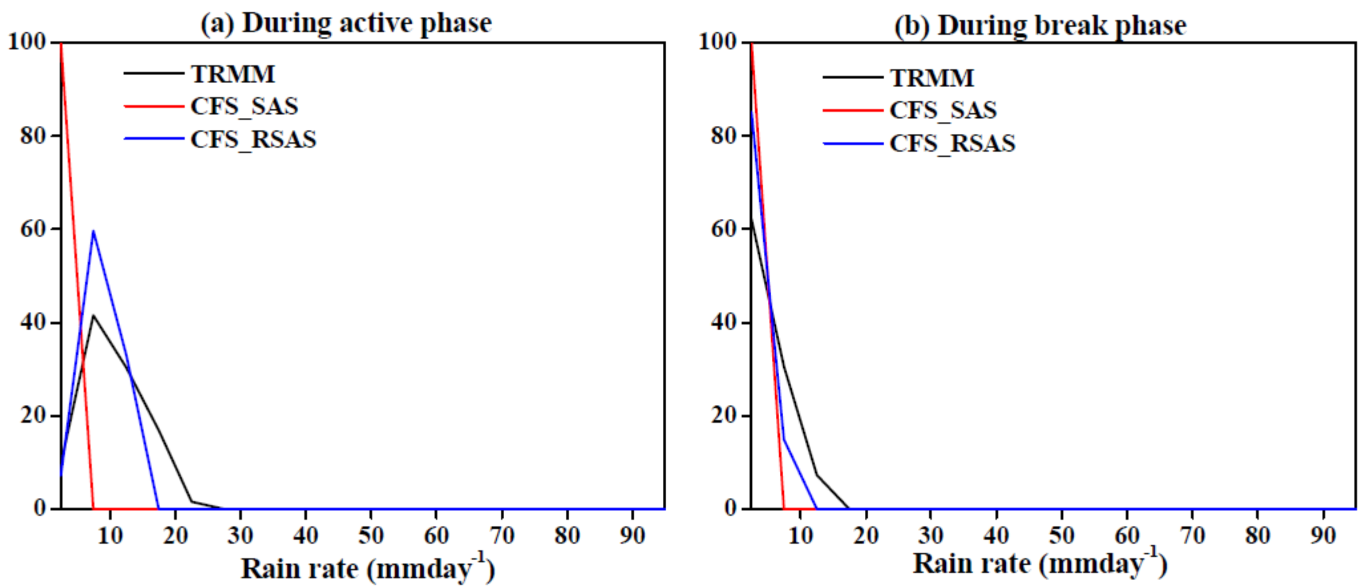

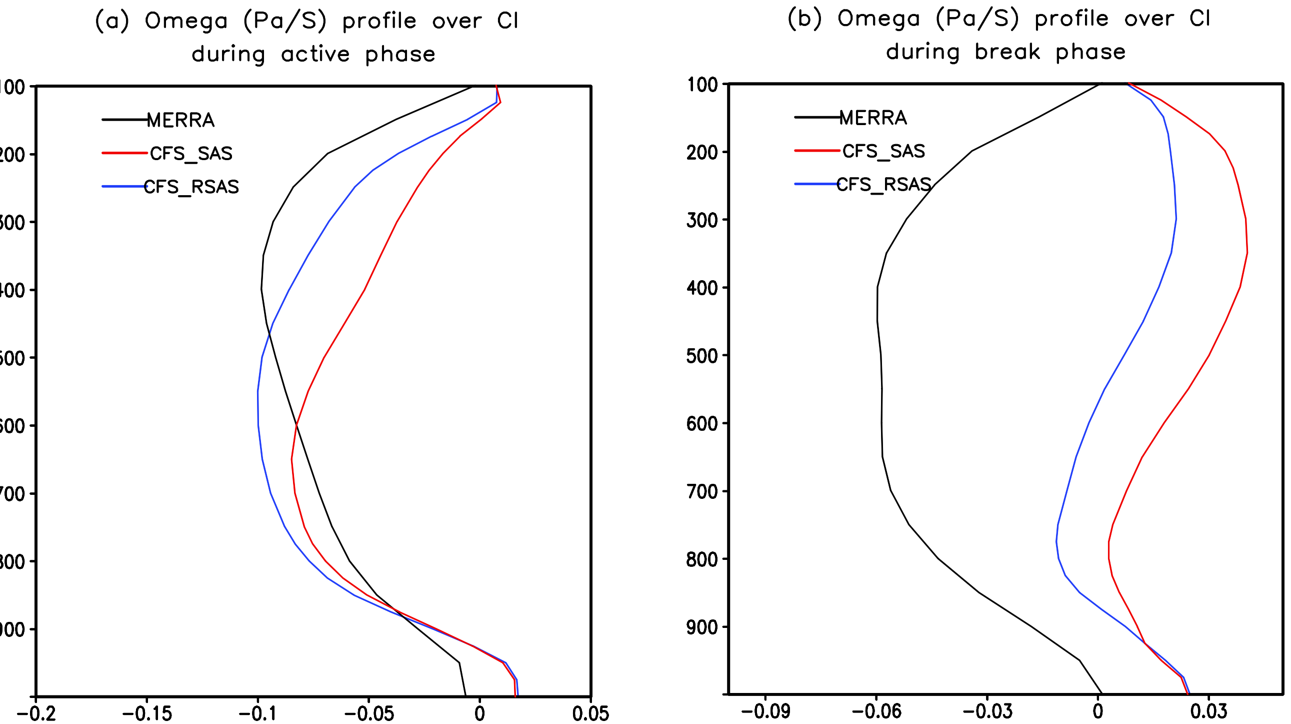
(a) Omega (Pa/S) profile over CI
during active phase
MERRA
CFS_SAS
CFS_RSAS
100
200
300
400
500
600
700
800
900
−0.2
−0.15
−0.1
−0.05
0
0.05
(b) Omega (Pa/S) profile over CI
during break phase
MERRA
CFS_SAS
CFS_RSAS
100
200
300
400
500
600
700
800
900
−0.09
−0.06
−0.03
0
0.03

Diurnal phase corresponding to maximum precipitation During ACTIVE phase

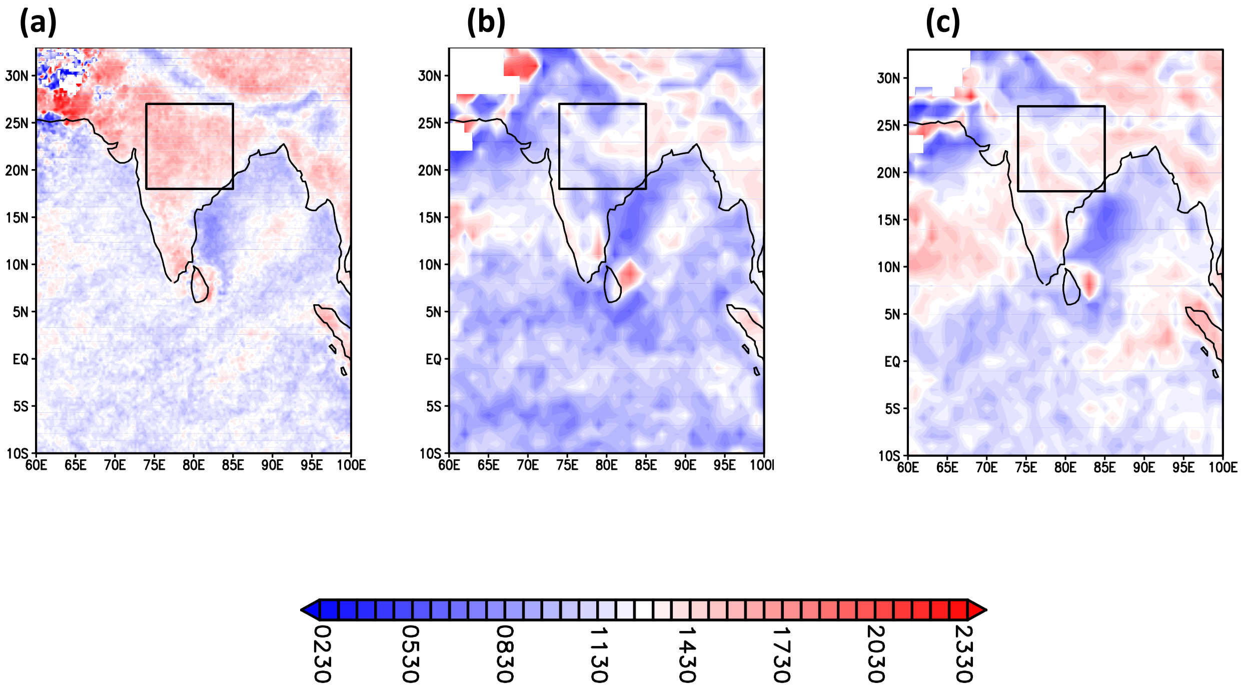

Diurnal phase corresponding to maximum precipitation
During BREAK phase

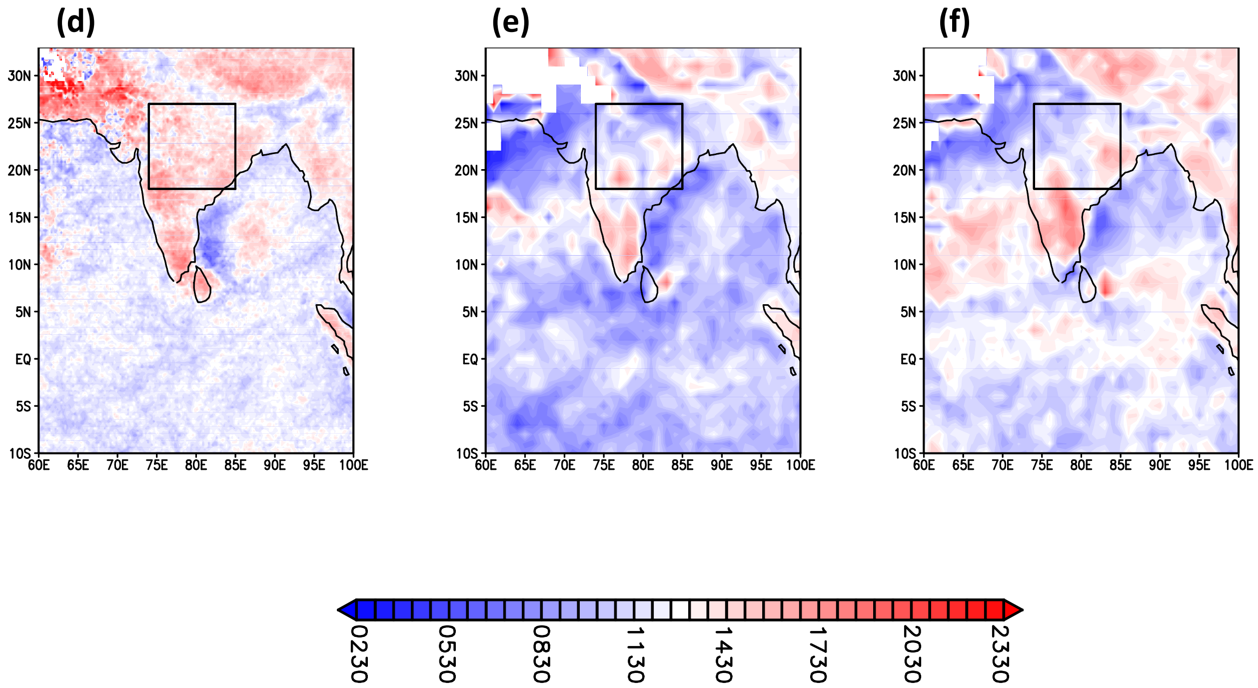

During Active (black lines) and Break (red lines) phases..

MERRA for CWMR, CIMR, TRMM for PRCP and Kalpana(solid line), Default SAS (dot dash line) and RSAS (dash line)

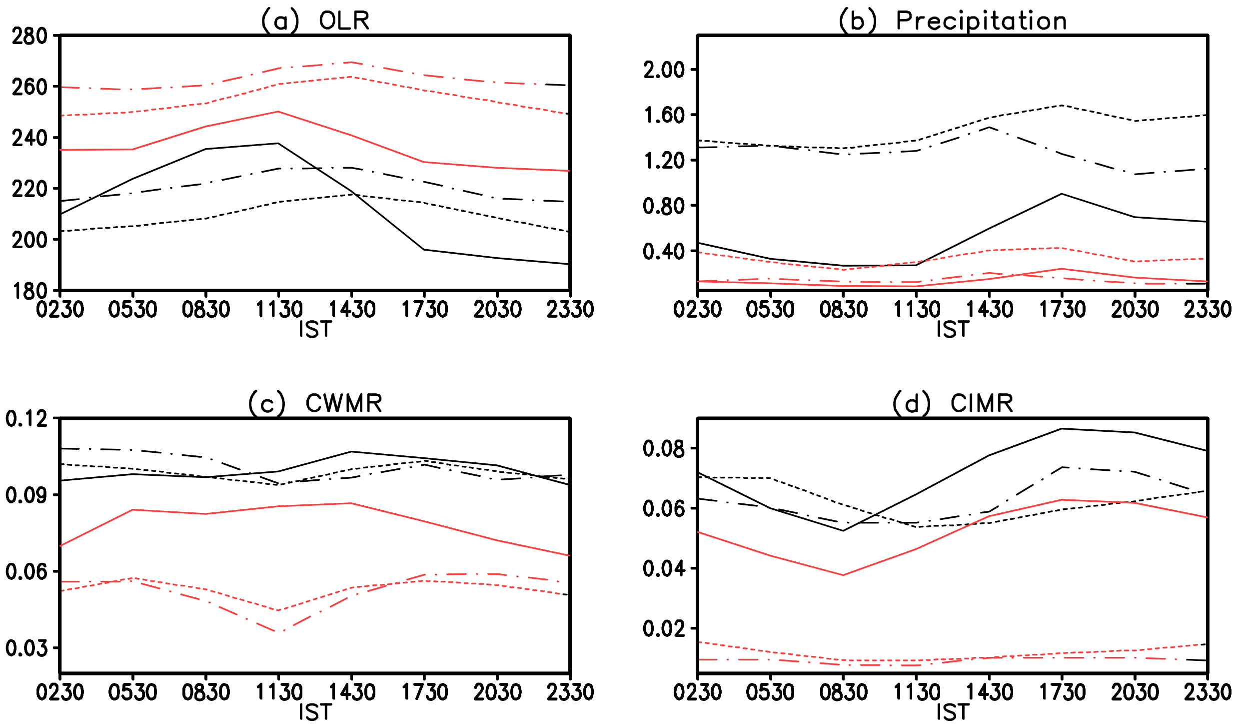

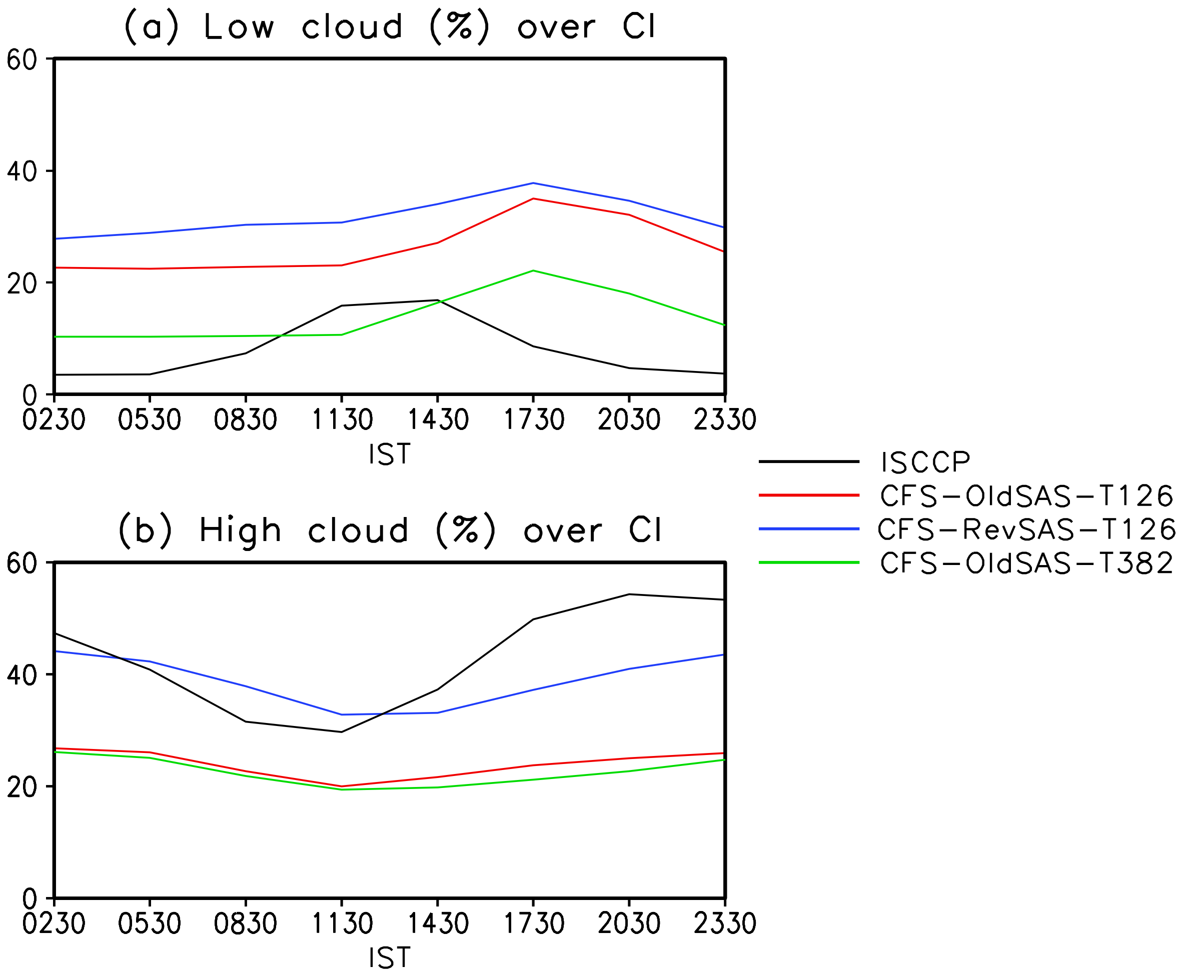

(a) Low cloud (%) over CI
60
40
20
0
0230 0530 0830 1130 1430 1730 2030 2330
IST
ISCCP
CFS−OldSAS−T126
CFS−RevSAS−T126
CFS−OldSAS−T382
(b) High cloud (%) over CI
60
40
20
0
0230 0530 0830 1130 1430 1730 2030 2330
IST

During Active (black lines) and Break (red lines) phases..

Default SAS (dot dash line) and RSAS (dash line)

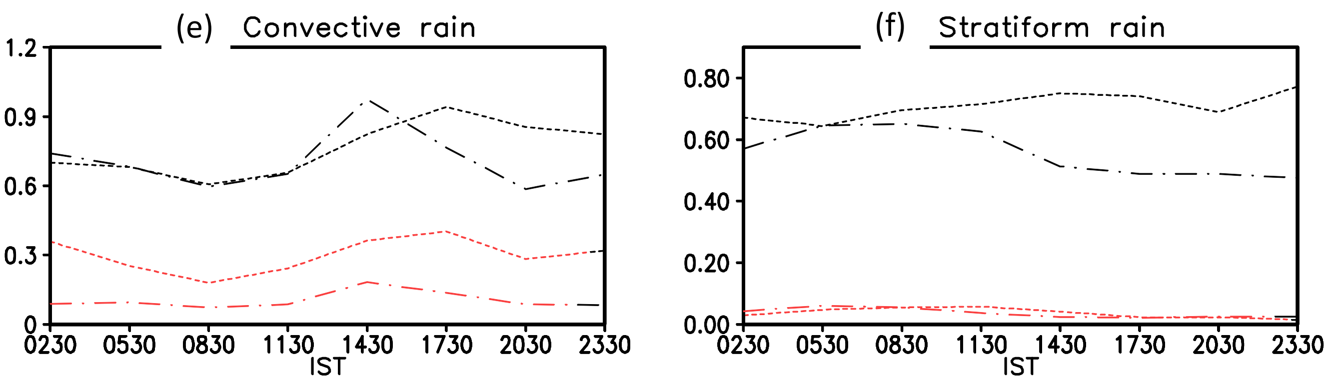

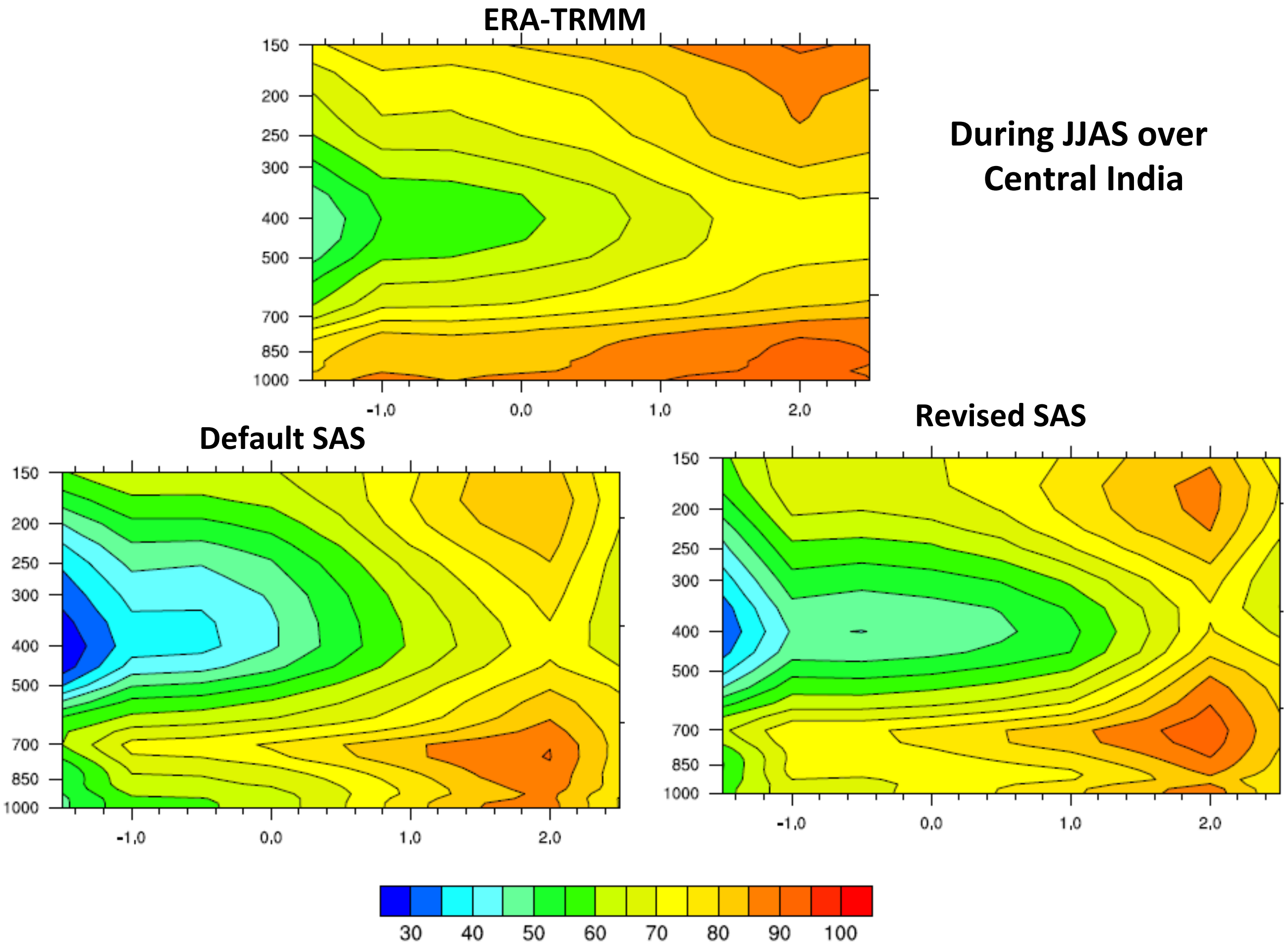
ERA-TRMM
During JJAS over Central India
Default SAS
Revised SAS
150
200
250
300
400
500
700
850
1000
-1.0
0.0
1.0
2.0
30
40
50
60
70
80
90
100

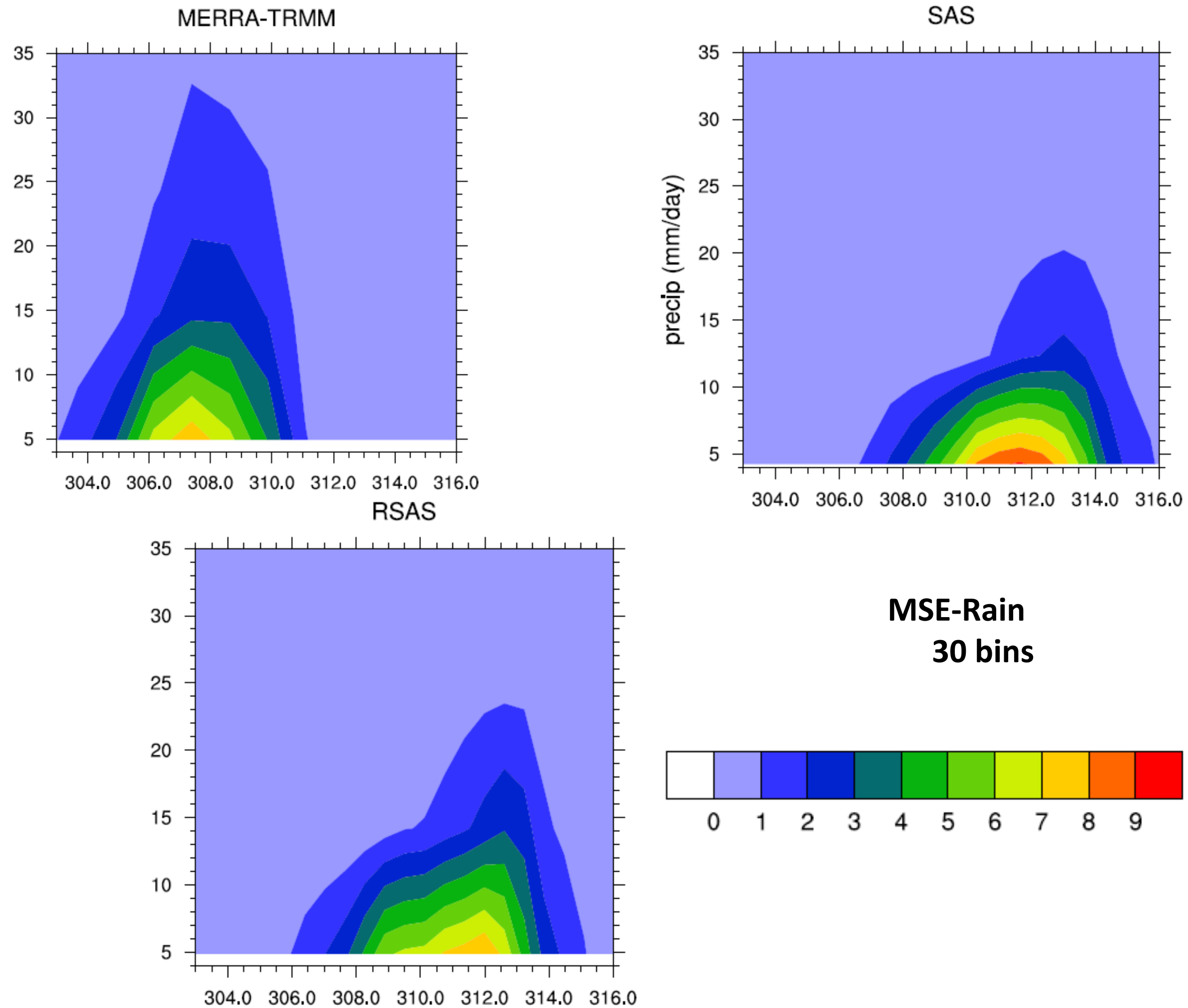

MERRA-TRMM
SAS
RSAS
precip (mm/day)
35
30
25
20
15
10
5
304.0
306.0
308.0
310.0
312.0
314.0
316.0
MSE-Rain
30 bins
0
1
2
3
4
5
6
7
8
9

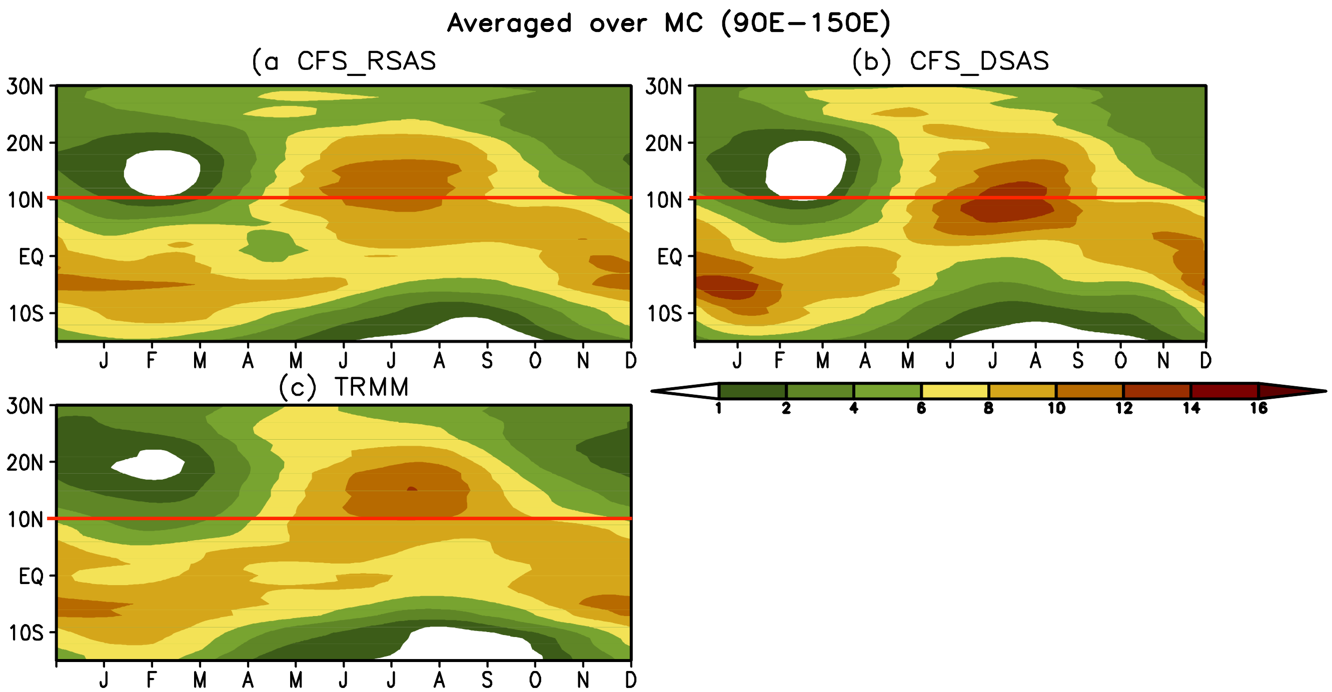
Averaged over MC (90E-150E)
(a CFS_RSAS
(b) CFS_DSAS
(c) TRMM
30N
20N
10N
EQ
10S
J F M A M J J A S O N D
1 2 4 6 8 10 12 14 16

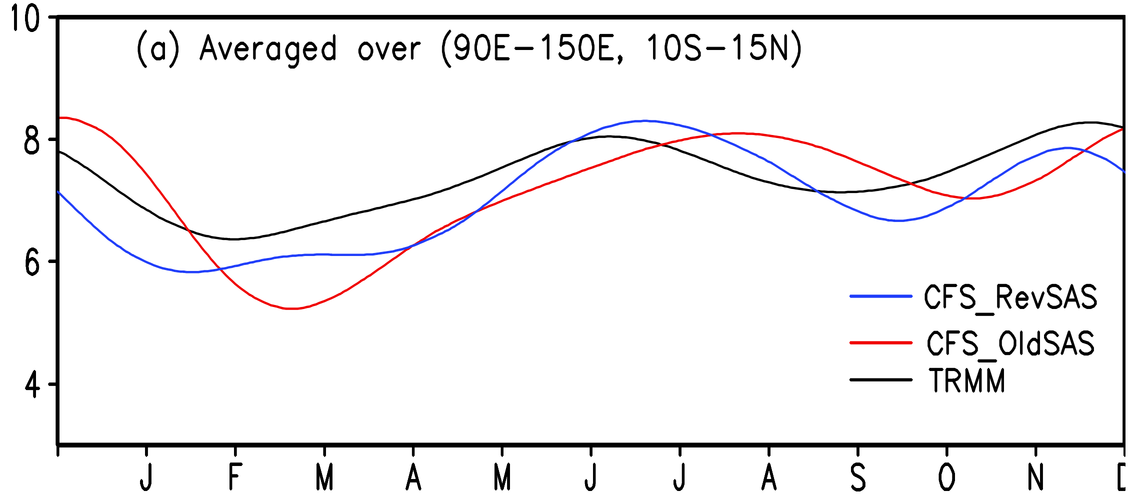

10
8
6
4
(a) Averaged over (90E-150E, 10S-15N)
CFS_RevSAS
CFS_OldSAS
TRMM
J
F
M
A
M
J
J
A
S
O
N
D

JJAS

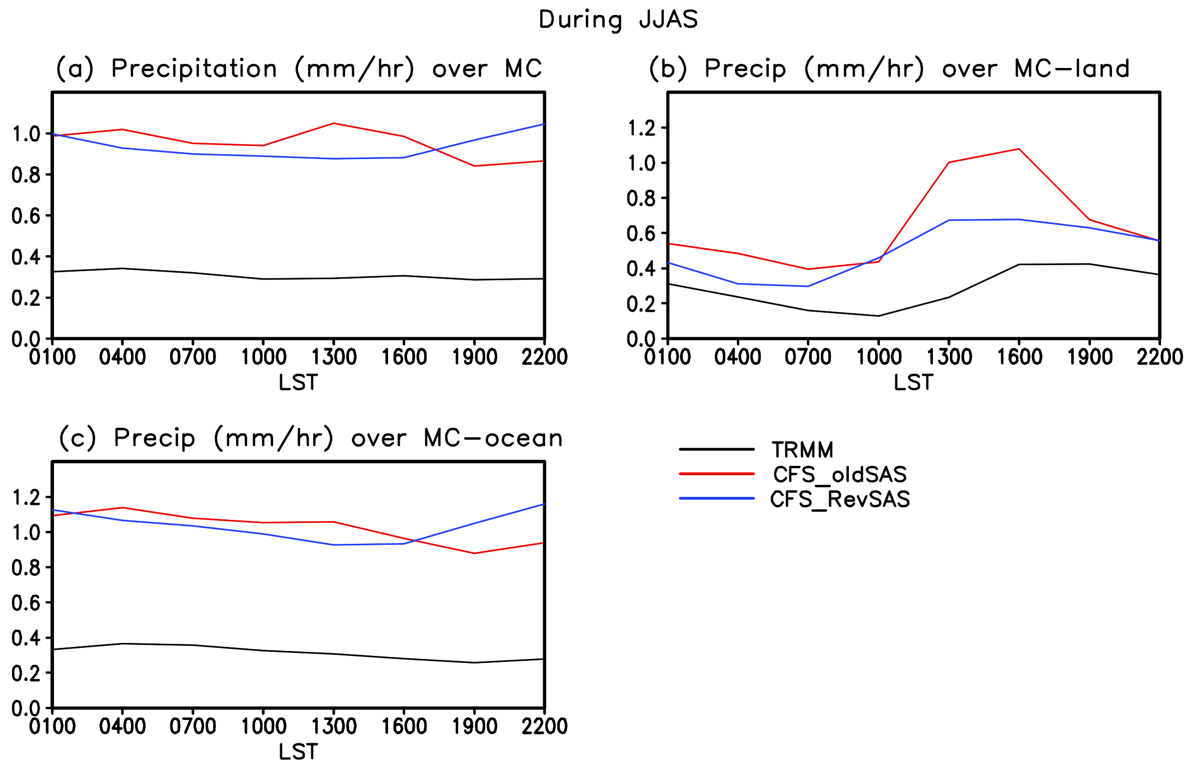
During JJAS
(a) Precipitation (mm/hr) over MC
1.0
0.8
0.6
0.4
0.2
0.0
0100 0400 0700 1000 1300 1600 1900 2200
LST
(b) Precip (mm/hr) over MC−land
1.2
1.0
0.8
0.6
0.4
0.2
0.0
0100 0400 0700 1000 1300 1600 1900 2200
LST
(c) Precip (mm/hr) over MC−ocean
1.2
1.0
0.8
0.6
0.4
0.2
0.0
0100 0400 0700 1000 1300 1600 1900 2200
LST
TRMM
CFS_oldSAS
CFS_RevSAS

Fig 12

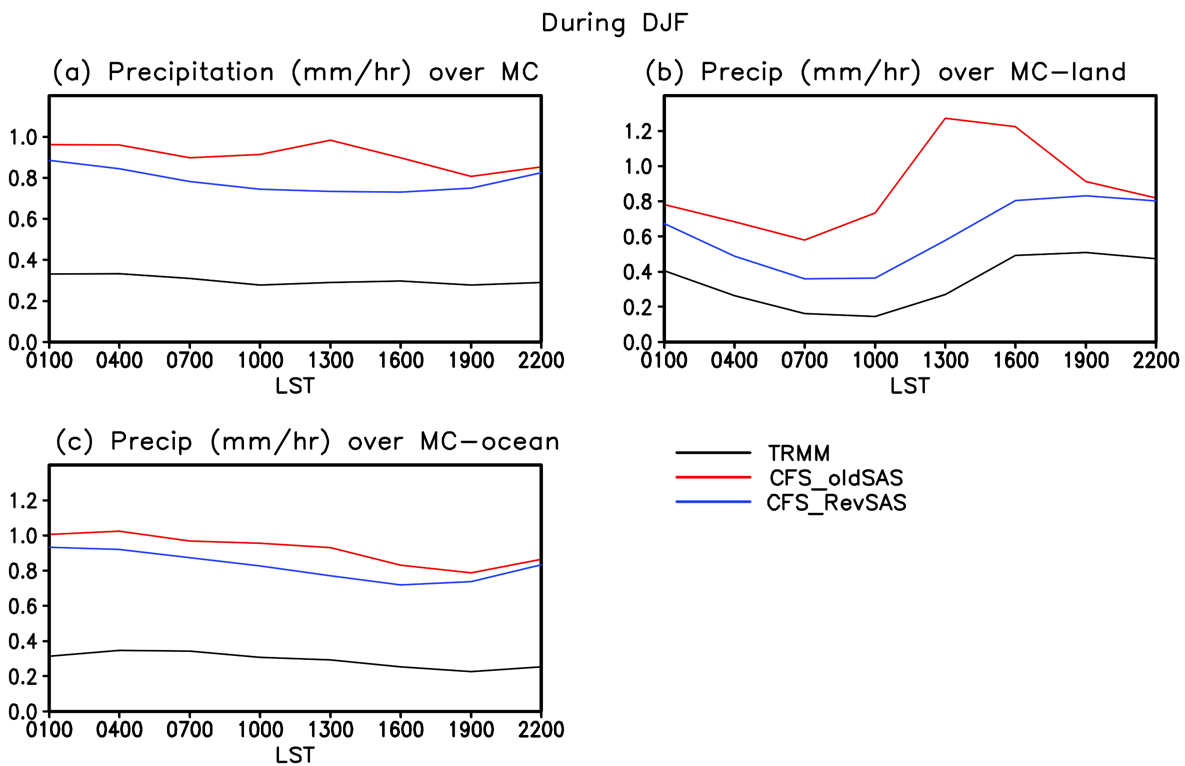
During DJF
(a) Precipitation (mm/hr) over MC
(b) Precip (mm/hr) over MC−land
(c) Precip (mm/hr) over MC−ocean
0.0
0.2
0.4
0.6
0.8
1.0
1.2
0100
0400
0700
1000
1300
1600
1900
2200
LST
TRMM
CFS_oldSAS
CFS_RevSAS

An Attempt with an Adjustment Scheme (BMJ) in GFS/CFS

Betts and Miller (1986) have defined three adjustment parameters, namely, the stability weight (Wt), which decides the slope of Tref profiles with respect to the moist adiabat; the saturation pressure departure (SPD) values, which are the measure of subsaturation; and the adjustment time period (t), which gives the time lag between the large-scale forcing and the convective adjustment. The qref profiles are constructed using the Tref profiles and the SPD values. The SPD values at three characteristic levels are prescribed. These are at cloud bottom (SPDb), at freezing level (SPDf), and at cloud top (SPDt). The SPD values at intermediate levels are linearly interpolated.

Vaidya and Singh, 2000, WAF

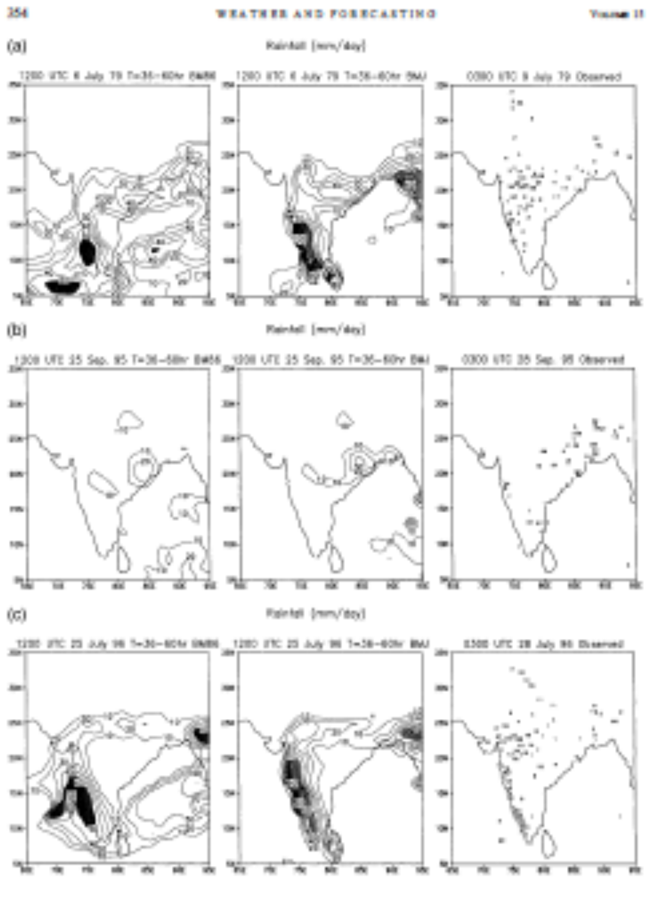

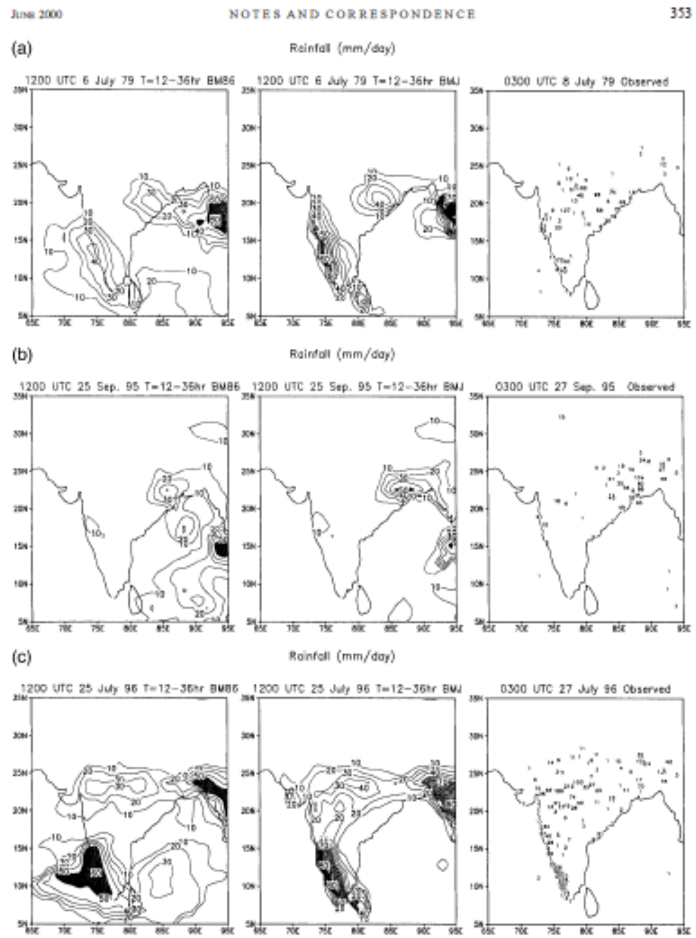

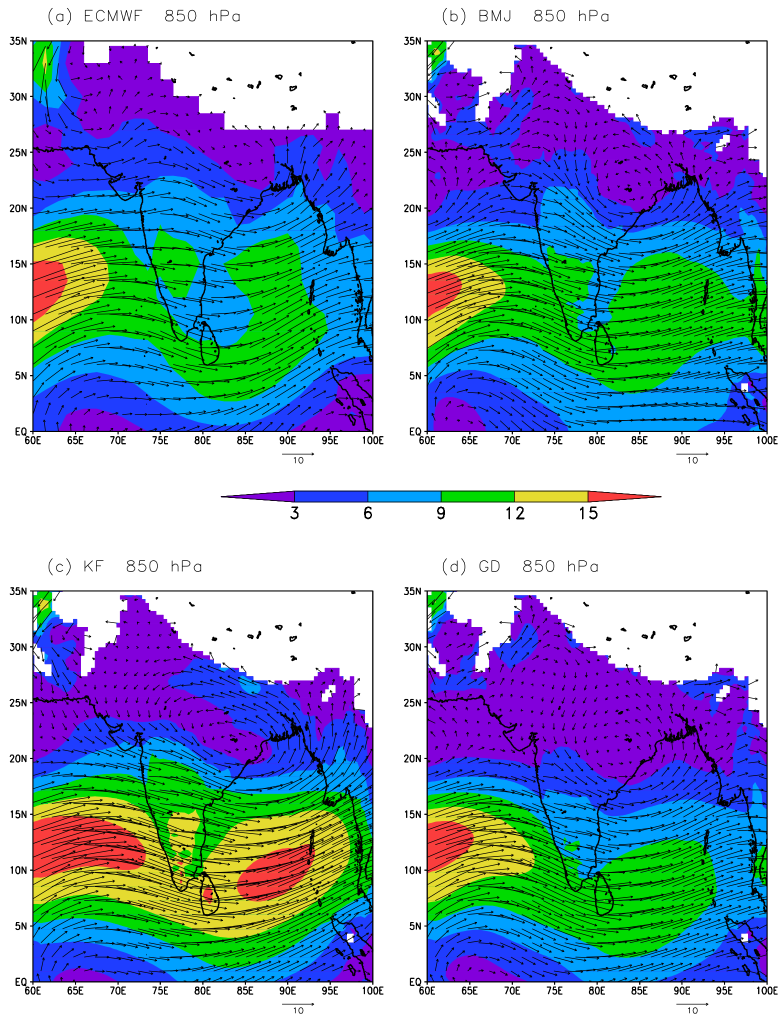

JJAS averaged mean 850 hPa wind (m/s) from (a) ECMWF, (b) BMJ, (c) KF and (d) GD for the year 2001-2007.

- KF has produced stronger low level southwesterly and corresponding horizontal cyclonic circulation than observations.
- GD on the other hand shows weaker than observations particularly over Bay of Bengal
- BMJ is in good agreement with the observation.

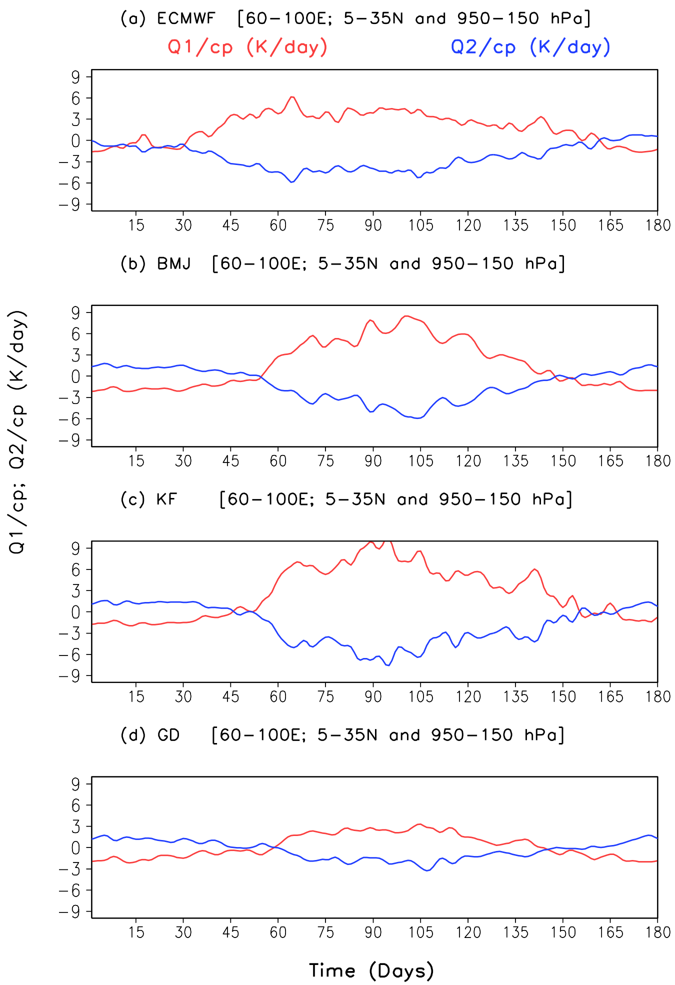

Seasonal evolution of apparent heat source (K/day), and moisture sink (K/day) averaged over 60-100°E and 5-35°N for the year 2001-2007 in (a) BMJ, (b) KF and (c) GD. The vertical integration is from 950-150 hPa.

- During winter and spring, Q_2 is negative and slowly increasing, suggesting stronger evaporation than precipitation. Soon after the onset, it starts to increase faster, but the evaporation continues to dominate because of the warm landmass, and about 2 pentads after the onset, precipitation overcomes evaporation (Xavier et al., 2007)
- The enhancement of precipitation overcoming evaporation after the monsoon onset and followed by maxima in the July-August and reduction of precipitation at the time of withdrawal is only reasonably captured by BMJ
- GD has hardly reproduced the seasonal variability of evaporation and condensation and both the processes are found to be comparable to each other throughout season
- KF could not reproduce the domination of evaporation over condensation at the time of withdrawal which means KF continues to produce rain even at the end of the season

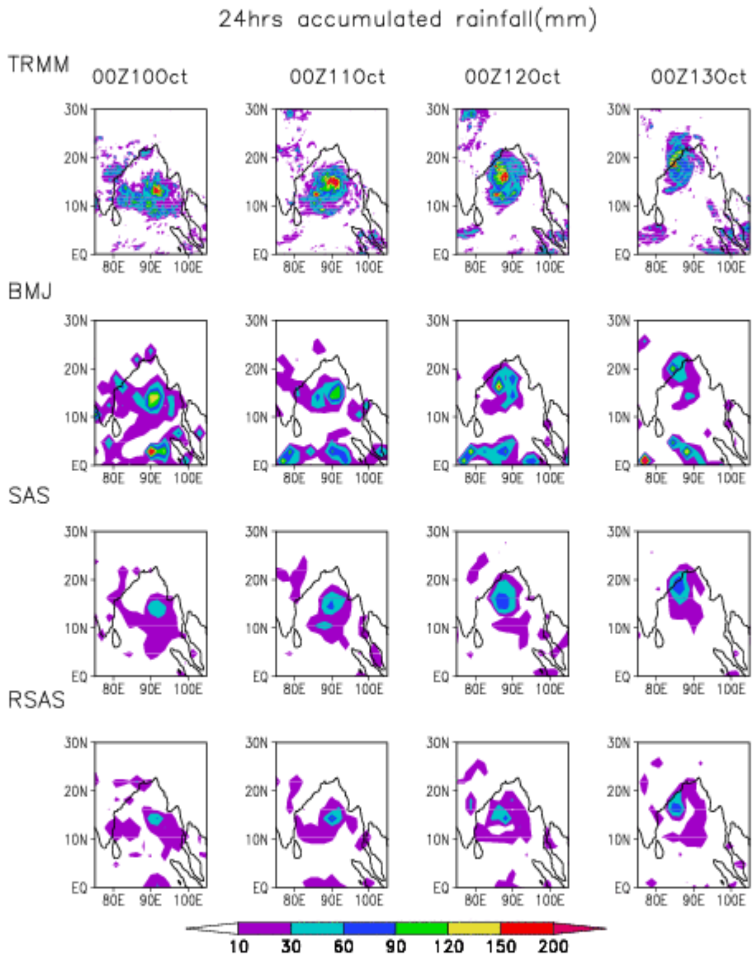
24hrs accumulated rainfall(mm)
TRMM
00Z10Oct
00Z11Oct
00Z12Oct
00Z13Oct
BMJ
SAS
RSAS
30N
20N
10N
EQ
80E
90E
100E
10
30
60
90
120
150
200

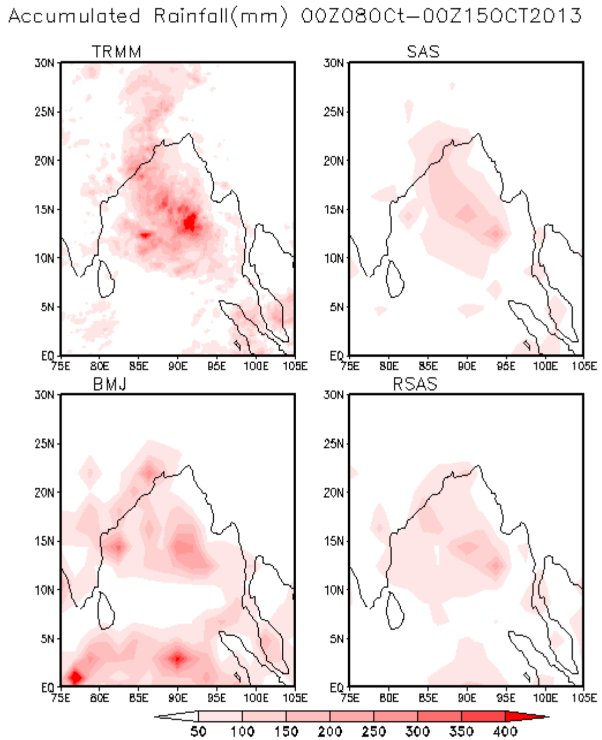
Accumulated Rainfall(mm) 00Z08Oct–00Z15OCT2013
TRMM
SAS
BMJ
RSAS
30N
25N
20N
15N
10N
5N
EQ
75E
80E
85E
90E
95E
100E
105E
50
100
150
200
250
300
350
400

MID LEVEL HEATING AND LOWER LEVEL VORTICITY

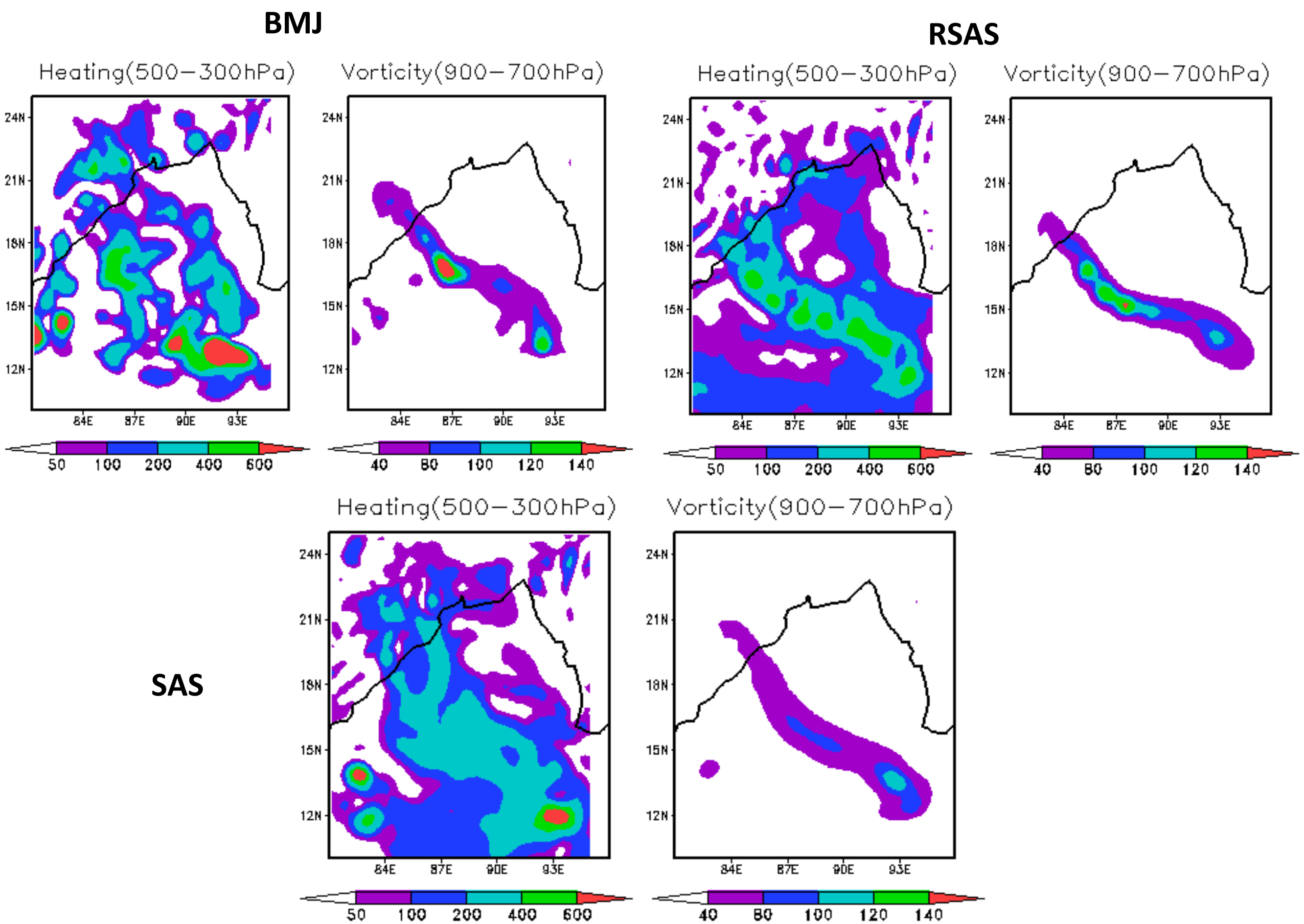

Vertically integrated MSE

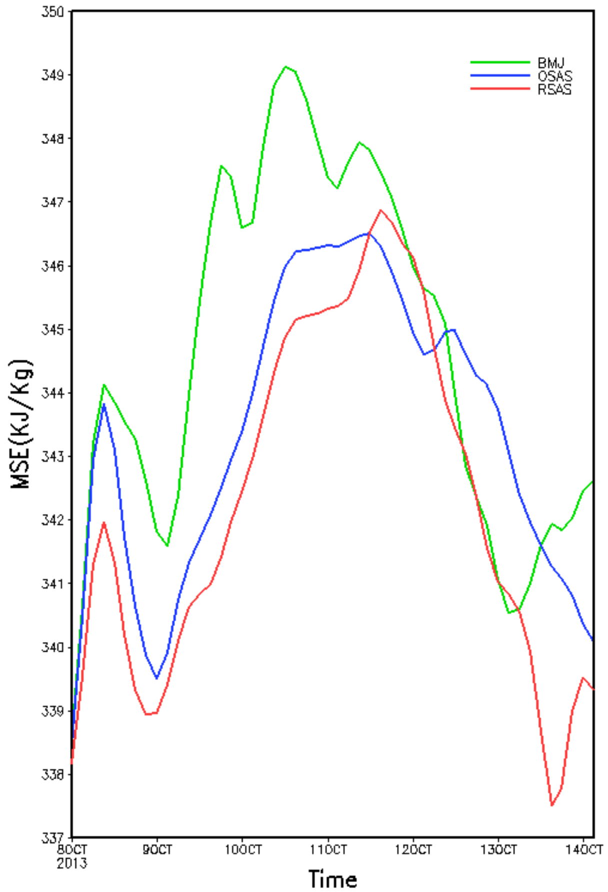

CFST382 (RED line), CFST126 (BLACK line), TRMM & MERRA (Dotted BLUE line)
OLR (INSAT) from Mahakur et al.

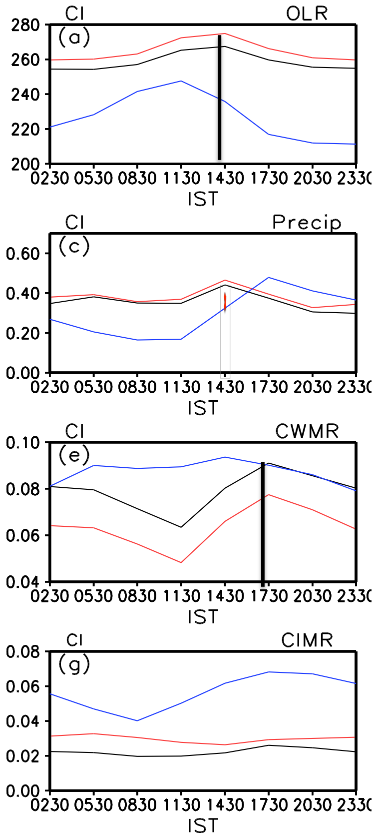

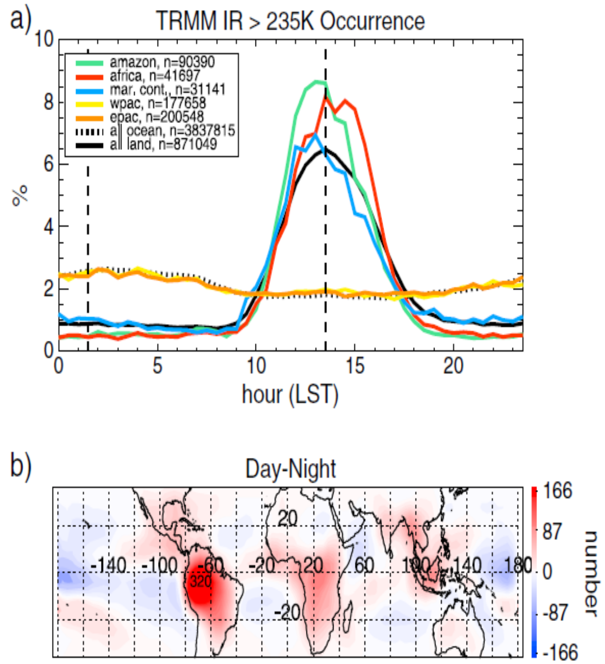

Diurnal variation of population of TRMM VIRS congestus for different regions. The black dashed lines indicate the times of CloudSat overpass.

Wall et al., 2013

Malay et al.

Diurnal variation of population of TRMM VIRS congestus for different regions over Indian monsoon region

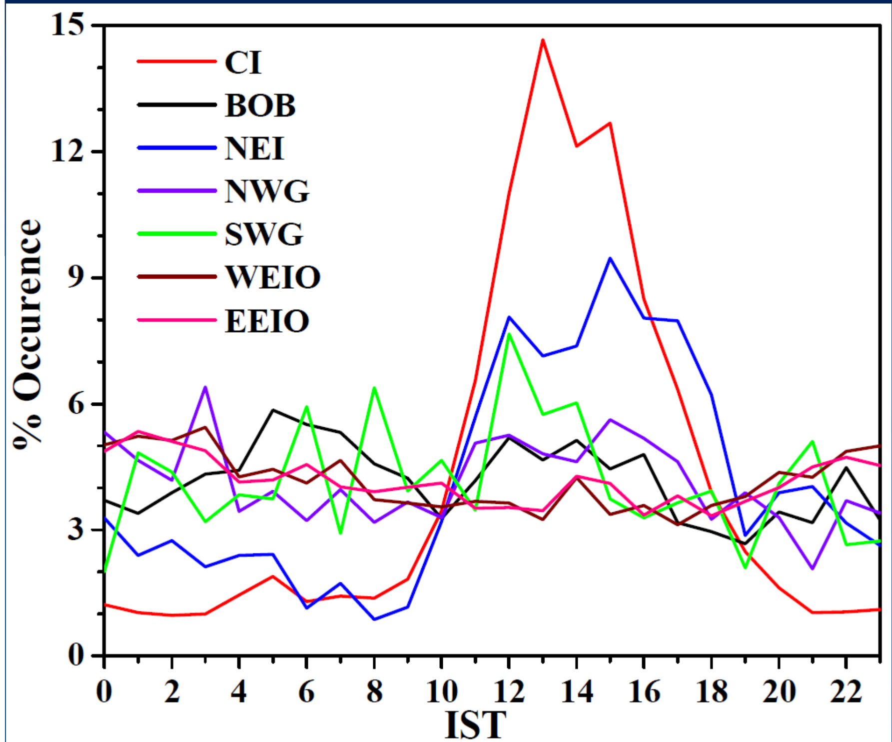

We hypothesize that the diurnal cycle of convection and hydrometeors need to be parameterized properly for improving diurnal precip

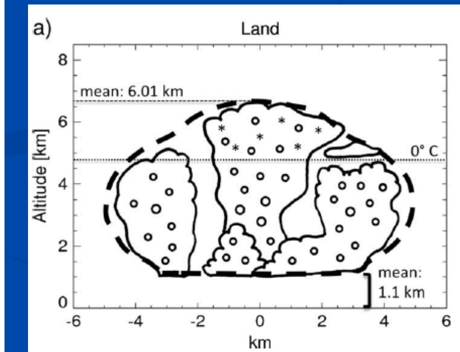

Mahakur et al.

Evaluating the Diurnal Cycle of Upper-Tropospheric Ice Clouds in Climate Models Using SMILES Observations

Jiang et al., 2015

Superconducting Submillimeter Limb Emission Sounder (SMILES) on the International Space Station (ISS)

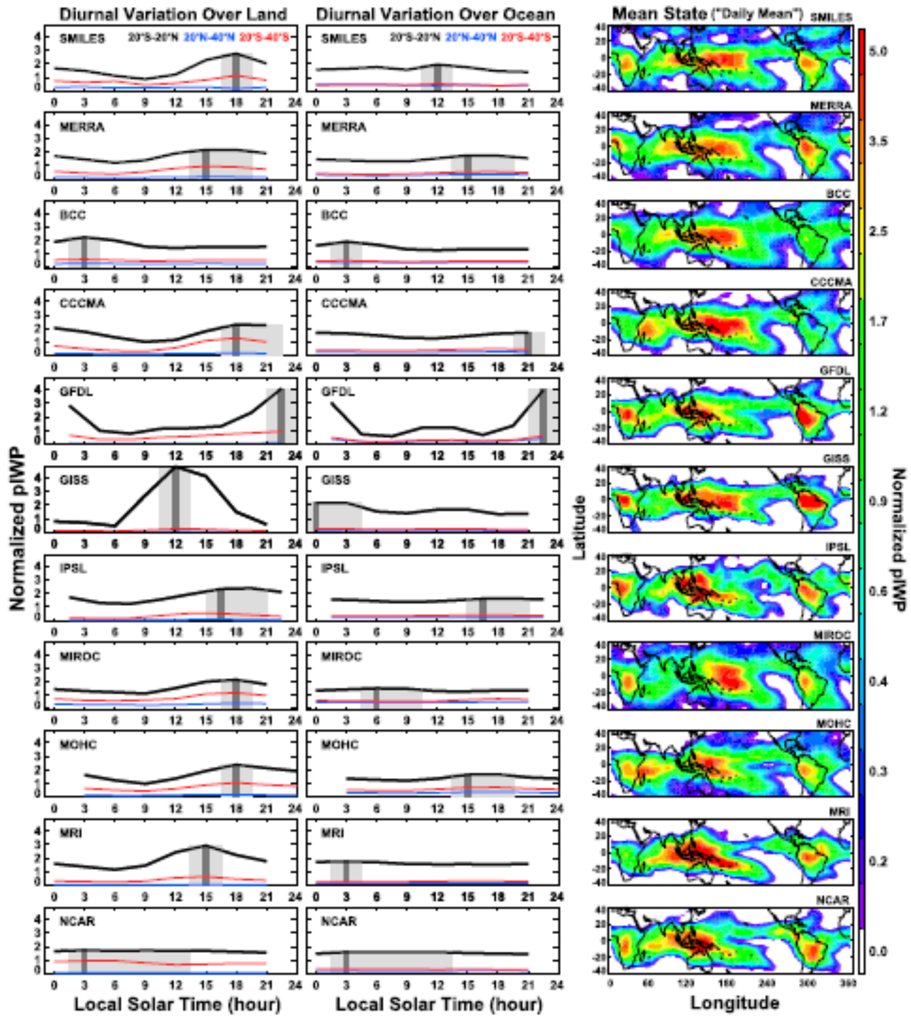

Fig. 8 Percentage of precipitation (averaged over SAM region, 10°N–30°N and 70°E–100°E) explained by convective (*red bars*) and stratiform (*blue bars*) types in the historical simulations of the 16 CMIP5 models along with that from observations (TRMM)

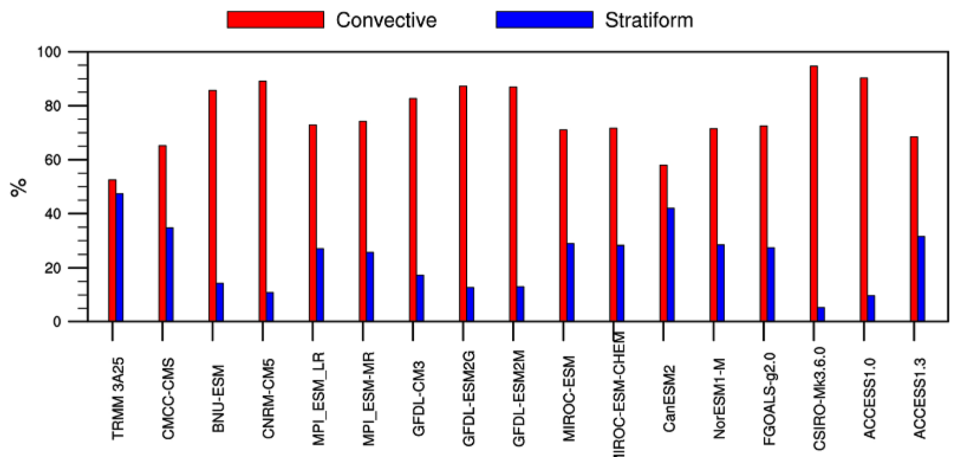

Why ensemble mean projection of south Asian monsoon rainfall by CMIP5 models is not reliable? C. T. Sabeerali · Suryachandra A. Rao · A. R. Dhakate ·K. Salunke · B. N. Goswami, Cli. Dyn. 2015

Revised convection, modified microphysics and radiation is able to improve the mean state and Intraseasonal variability of CFSv2T126

Annual Rainfall Cycle
<73°-85°E, 15°-25°N>

<40°-120°E, 15°S-30°N>

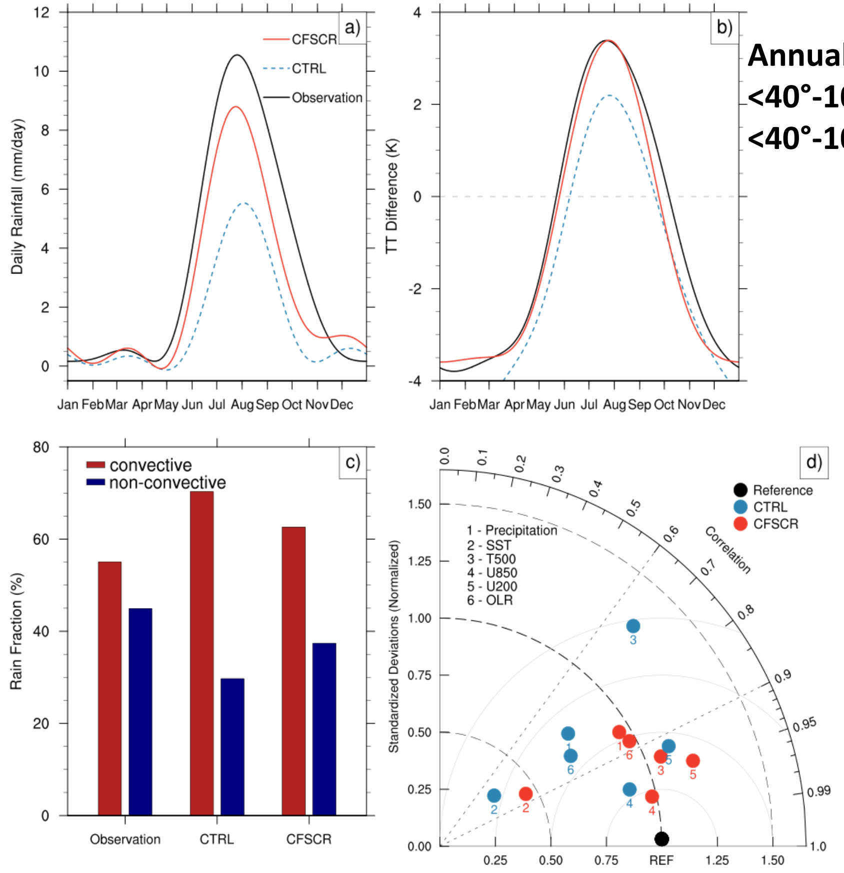

Annual TT Difference
<40°-100°E,5°-35°N> - <40°-100°E,15°S-5°N>

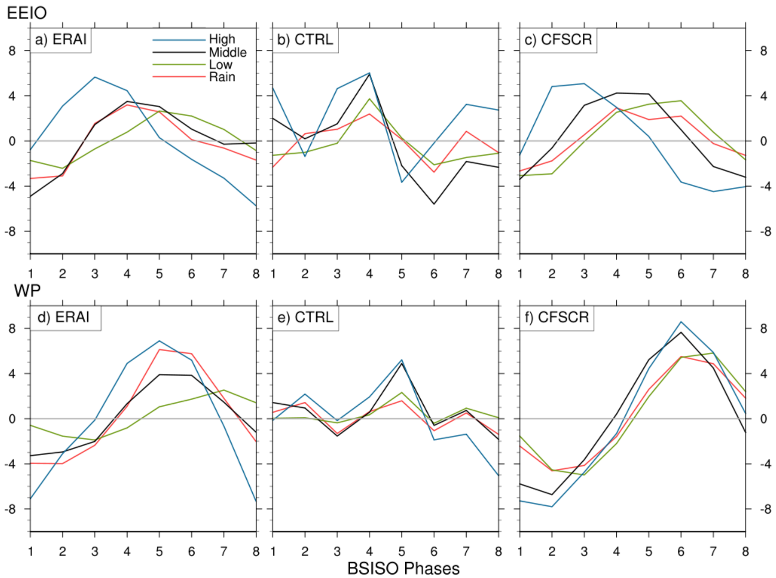

Evolution of anomalous low, middle and high cloud fractions (%, left axis) and rainfall anomalies (mm day-1, right axis) associated with BSISO1 convection over EEIO (top panels) and WP (bottom panels) for (a-b) observation, (c-d) CTRL and (e-f) CFSCR.

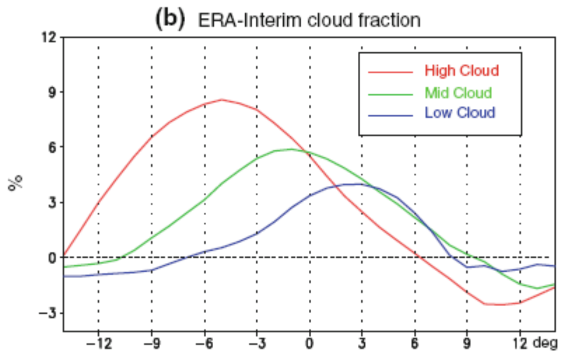

Jiang et al. 2011

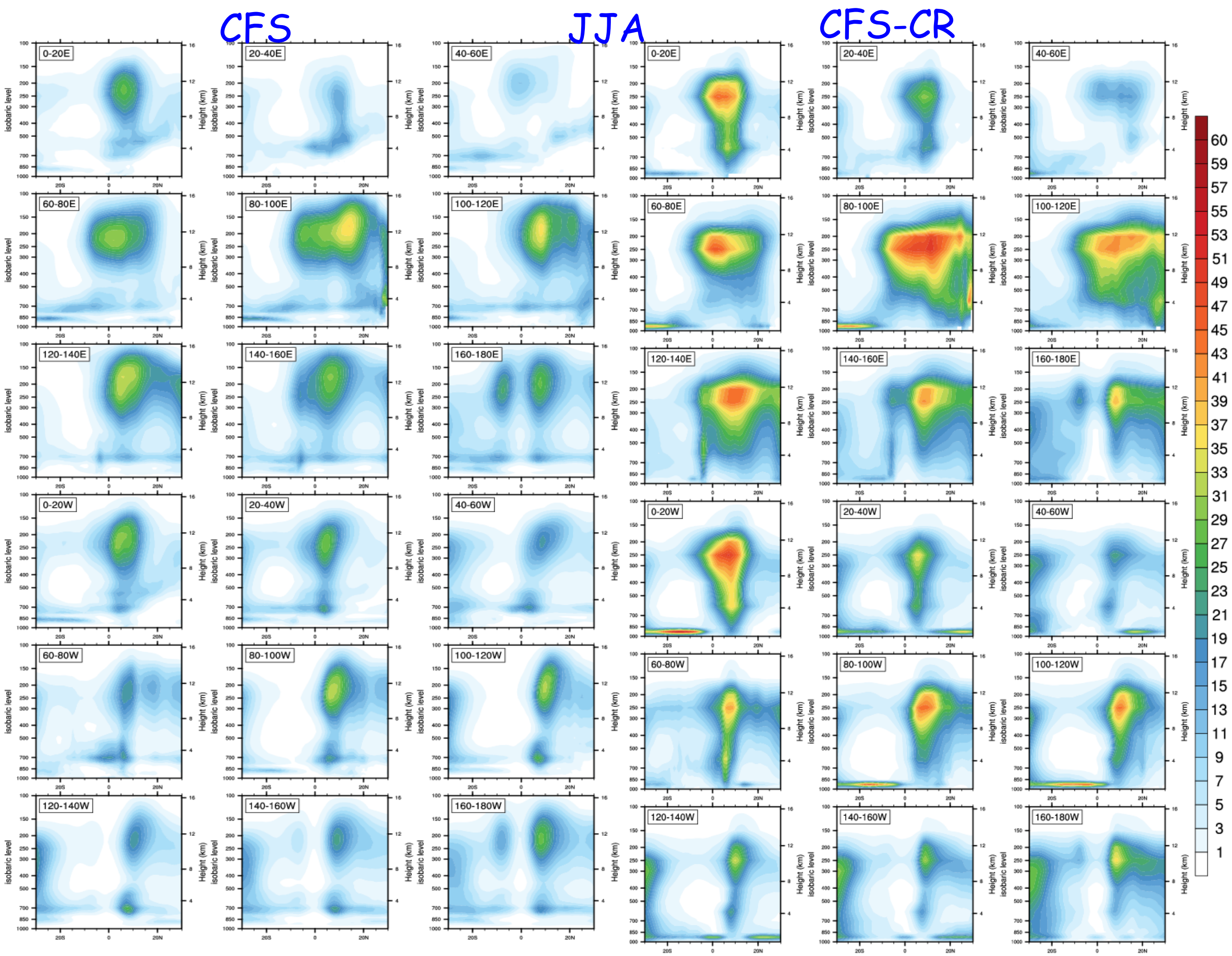

CFS
JJA
CFS-CR
0-20E
20-40E
40-60E
60-80E
80-100E
100-120E
120-140E
140-160E
160-180E
0-20W
20-40W
40-60W
60-80W
80-100W
100-120W
120-140W
140-160W
160-180W
isobaric level
Height (km)
20S
0
20N
60
59
57
55
53
51
49
47
45
43
41
39
37
35
33
31
29
27
25
23
21
19
17
15
13
11
9
7
5
3
1

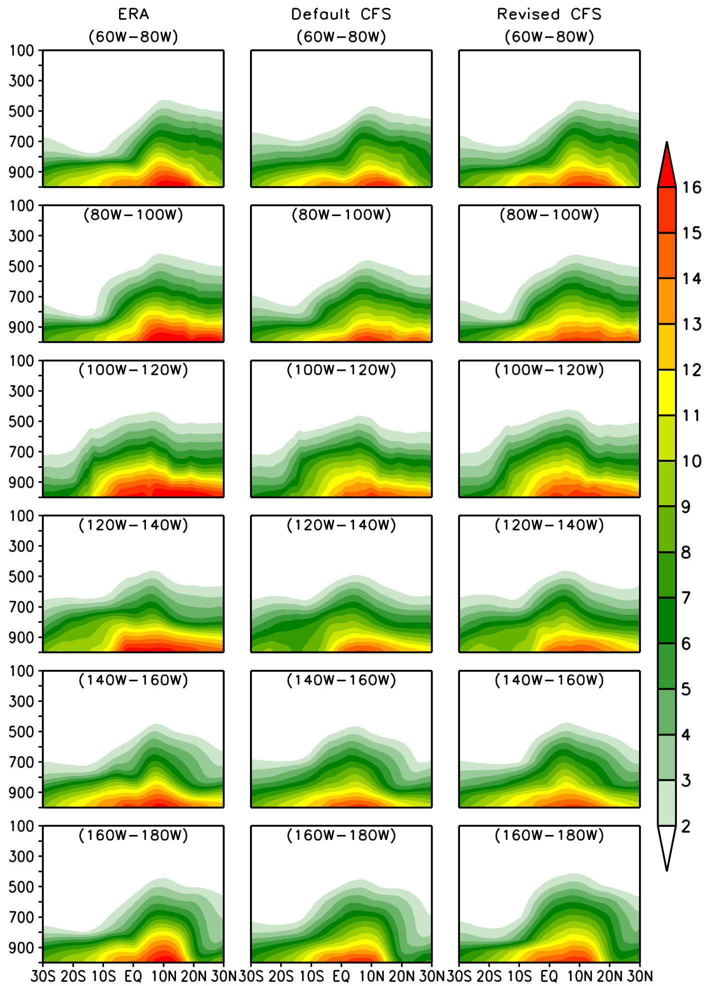

JJA MEAN Vert. distribution of Sp. humidity

Moncrieff et al, 2012, BAMS

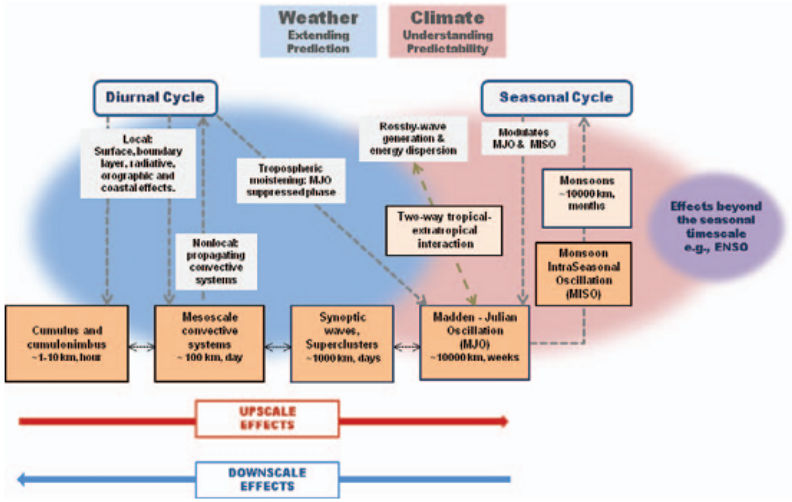

Scientific Basis of the study

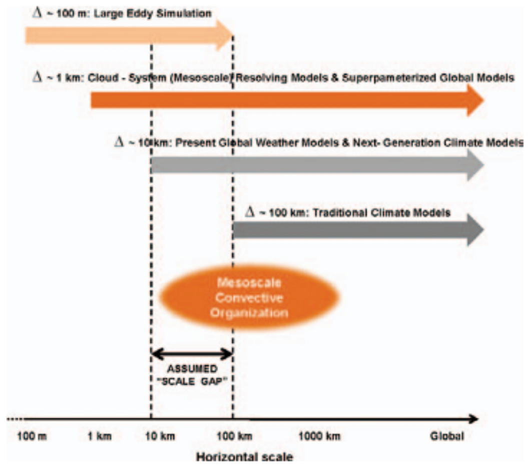

The organized systems exhibit hierarchical coherence: (i) mesoscale systems consist of families of cumulonimbus; (ii) cumulonimbus and MCS are embedded in synoptic waves; and (iii) the MJO/MISO is an envelope of cumulonimbus, MCS, and superclusters.
The upscale effects of convective organization are not represented in traditional climate models.
The mean atmospheric state exerts a strong downscale control on convective structure, frequency, and variability. Mesoscale convective organization bridges the scale gap assumed in traditional convective parameterization.

- **(i) SCM/CRM resolves cumulus, cumulonimbus, mesoscale circulations, but the computational domain is small (~100 km) and simulations short (~1 day).**
- **(ii) Two-dimensional CSRMs in superparameterized global models permit MCS-type organization and mesoscale dynamics.**
- **(iii) High-resolution global numerical prediction models may crudely represent large MCS (superclusters). (iv) MCS, and other mesoscale dynamical systems, are absent from traditional climate models—organized convection is not parameterized.**

Summary

- Fractional entraiment and detrainment ad the mass flux estimate constrained by LES studies has helped the convection to improve the diurnal variation over ISM and also over Maritime continent region.

- The adjust scheme of BMJ, shows promise in improving the moist instability, instability, voriticity associated with strong convective system e. g. Tropical cyclone.

- Inclusion of robust cloud processes at grid scale has helped CFSv2 to capture the cloud phases across the globe mostly due to improved moist process and improve the convective/stratiform distribution.

- Further efforts are needed to incorporate the multiscale convection (Cumulus, mesoscale, synoptic and ISO/MJO)

Thank You !

INDIAN INSTITUTE OF TROPICAL METEOROLOGY PUNE